Structure-Based Virtual Screening, Molecular Docking, Molecular Dynamics Simulation of EGFR for the clinical treatment of Glioblastoma

Aditi Pande
Eminent Biosciences
Mohnad Abdalla
Shandong University School of Medicine: Shandong University Cheeloo College of Medicine
Maddala Madhavi
Osmania University
Ishita Chopra
Eminent Biosciences
Anushka Bhrdwaj
Eminent Biosciences
Lovely Soni
Eminent Biosciences
Natchimuthu Vijayakumar
Eminent Biosciences
Umesh Panwar
Eminent Biosciences
Mohd. Aqueel Khan
Alagappa University
Leena Prajapati
Eminent Biosciences
Deepika Gujrati
Osmania University
Pranoti Belapurkar
Acropolis Institute
Sarah Albogami
Taif University
Tajamul Hussain
King Saud University College of Science
Chandrabose Selvaraj
Alagappa University
Anuraj Nayarisseri (anuraj@eminentbio.com)

In silico Research Laboratory, Eminent Biosciences, Vijaynagar, Indore –India. https://orcid.org/0000-0003-2567-9630

Sanjeev Kumar Singh

Alagappa University

Research Article

Keywords: EGFR, Glioblastoma, Virtual Screening, Molecular Docking, MD Simulation, R Programming, ADMET, Boiled Egg Plot.

Posted Date: June 7th, 2022

DOI: https://doi.org/10.21203/rs.3.rs-1536497/v2

Abstract

Glioblastoma (GBM) is a WHO Grade IV tumor with poor visibility, a high risk of comorbidity, and limited treatment options. Resurfacing from second-rate glioma was originally classified as either mandatory or optional. Recent interest in personalized medicine has motivated research toward biomarker stratification-based individualized illness therapy. GBM biomarkers have been investigated for their potential utility in prognostic stratification, driving the development of targeted therapy, and customizing therapeutic treatment. Due to the availability of a specific EGFRvIII mutational variation with a clear function in glioma-genesis, recent research suggests that EGFR has the potential to be a prognostic factor in GBM, while others have shown no clinical link between EGFR and survival. The pre-existing pharmaceutical lapatinib (PubChem ID: 208908) with a higher affinity score is used for Structure-based Virtual Screening. As a result, the current study revealed a newly screened chemical (PubChem CID: 59671768) with a higher affinity than the previously known molecule. When the two compounds are compared, the former has the lowest re-rank score. The time-resolved features of a virtually screened chemical and an established compound were investigated using Molecular Dynamics Simulation. Both compounds are equivalent, according to the ADMET study. This report implies that the virtual screened chemical could be a promising Glioblastoma therapy.

1. Introduction

Glioblastoma (GBM) is a WHO Grade IV tumor with poor visibility, significant comorbidity, and limited treatment options. It was initially classified as either essential, emerging again, or optional, emerging from second-rate glioma. Glioma genesis has been shown to be influenced by transformations required for the characterization of these tumors[1]. O-6-methylguanine-DNA-methyltransferase (MGMT), isocitrate dehydrogenase quality 1 and 2 (IDH1/2), p53, epidermal development factor receptor (EGFR), platelet-determined development factor receptor (PDGFR), phosphatase and tensin homolog (PTEN), phosphoinositide 3-kinase (PI3K), and 1p/19q are some of the genes involved in GBM tumor. These characteristics serve as biomarkers of illness severity, provide insight into the pathogenesis of the disease, and may serve as potential targets for targeted therapy. We designed to analyze the clinical impact of these quality markers on necrotic tissue, as well as how they influence forecasting and clinical dynamics for regular clinicians, in this study [2–3]. The Epidermal Growth Factor Receptor will be the focus of this research [4–5].

EGFR is a cell surface-bound receptor that plays a role in cell proliferation and may have implications for GBM clinical outcomes. EGFR mutations are found in about half of primary GBMs and ten percent of secondary GBMs[7]. Furthermore, the EGFR variation III mutation (EGFRvIII) with a deletion of the regulator N-terminal domain (6-273) is found in 10–60% of initial GBMs, resulting in constitutive activation of mitogenic signaling pathways. (7)Other EGFR mutation types exist, but their clinical importance is unknown (for example, the C-terminal domain [C]-958, intergenic deletions [D521–603], duplication-insertion mutations [664–1030 and 664–1014]). EGFRvIII can be detected in the peripheral blood of brain tumor patients, allowing for screening and tracking of response to anti-EGFRvIII therapy [7].

The EGFR (ErbB1) protein is involved in the control of normal cell development. EGFR belongs to the ErbB receptor family, which also includes three additional members. Extracellular space is involved in ligand official, whereas intracellular signaling includes cytosolic space[8]. The EGFR acts as a receptor protein kinase. When a ligand binds to EGFR, it causes it to dimerize and form a dynamic homodimer or heterodimer with other ErbB receptors [9]. As a result, cell growth, proliferation, migration, and adhesion are stimulated, whereas apoptosis is inhibited.

Three receptor protein kinases, including JAK2, wild-type EGFR, and EGFRvIII, can phosphorylate STAT3 in GBM [10]. This phosphorylation causes this prooncogenic transcription factor to be activated indefinitely. The tumor suppressor - Phosphatase and Tensin Homolog (PTEN) can prevent STAT3 activation. PTEN is inactivated in a large percentage of GBM cells due to gene mutations or deletion. STAT3 plays a role in GBM pathogenesis by stimulating the tumorigenic transcriptional pathway [Fig. 1] [11–15]. STAT3 can up-regulate the production of inducible nitric oxide (NO) synthase (iNOS) in EGFRvIII-expressing astrocytes, and iNOS activity increases glioma stem cell proliferation and tumorigenicity. The activation of cyclooxygenase-2 (COX2) transcription requires the upregulation of STAT3 by EGFR/EGFRvIII. COX2 is involved in the control of growth, propagation, and neo-vascular development in cells, as well as the creation of prostaglandins. Normal cells undergo an epithelial-mesenchymal transition (EMT) when TWIST is activated by STAT3 [16–18]. Hypoxia upregulates STAT3 in glioblastoma cell lines, resulting in enhanced angiogenesis and tumor cell migration [19–20]. STAT3 stimulates VEGF expression in GBM patients. In participants with newly diagnosed GBM, there was a direct link between STAT3 expression and the expansion of vasogenic cerebral edema [21–26].

Through activation of the urokinase plasminogen activator (uPA)-UPAR-Erk1/2 [27–33]signaling and further down-regulation of the proapoptotic protein BIM, EGFRvIII has been found to limit apoptosis in glioblastoma cells [34–35]. In medulloblastomas, it was discovered that EGFR-induced STAT3 is implicated in the up-regulation of uPA and matrix metalloproteinase (MMP)-9, as well as apoptosis suppression. Activated STAT5 was discovered to form a complex within the nucleus of glioblastoma cells, which primes the transcription of target genes such as the anti-apoptotic Bcl-XL. STAT-3 signaling generated by EGFRvIII may also have a role in the development of other cancers, such as breast carcinoma. [36–40]The goal of this work is to find an effective compound that can inhibit the activity of EGFR in glioblastoma cells by disrupting the urokinase plasminogen activator (uPA)-UPAR-Erk1/2 signaling pathway.

2. Results

2.1 Pre-processing & Docking results

Obtained crystal coordinates of an extracellular region of EGFR and PubChem compounds were pre-processed for molecular docking studies. The best-established compound was Lapatinib (PubChem ID: 208908) based on docking tests of complete pre-established 16 medicines [Table 2]. Lapatinib has a high-affinity score for our target protein, with a molecular weight of 581.058 g/mol, a hydrogen bond

donor count of 2 and a hydrogen bond acceptor count of 9, a topological polar surface area of 115A2, and a logP value of 5.9. In Glioblastoma, the chemical Lapatinib exhibits a higher inhibitory affinity on the protein EGFR.

Table 1
List of inhibitors by survey of literature.

Inhibitor	Pub ID	MW	HBD	HBA	LogP	ref no.
Gefitinib	123631	446.9 g/mol	1	8	4.1	33
Erlotinib	176870	393.4 g/mol	1	7	3.3	34
Lapatinib	208908	581.1 g/mol	2	9	5.9	35
capecitabine	60953	359.35 g/mol	3	7	0.6	36
cyclopamine	442972	411.6 g/mol	2	3	3.5	38
Afatinib	10184653	485.9 g/mol	2	8	3.6	39
Temozolomide	5394	194.15 g/mol	1	5	-1.1	40
carmustine	2578	214.05 g/mol	1	3	1.5	41
Cetuximab	91820602	354.3 g/mol	2	3	4	42
Dacomitinib	11511120	469.9 g/mol	2	7	4.4	43
AEE788	10297043	440.6 g/mol	2	5	4.6	45
Tarceva (OSI-774)	176870	393.4 g/mol	1	7	3.3	46
Temodar	5394	194.15 g/mol	1	5	-1.1	47
carboplatin	426756	371.25 g/mol	4	6	0.4	48
procarbazine	4915	221.3 g/mol	3	3	0.1	49
vandetinib	3081361	475.4 g/mol	1	7	4.9	50

Table 2
Docking results of established compounds against EGFR.

PubChem ID	MolDock Score	Rerank Score	HBond	MW
208908	-151.764	-113.707	-4.15386	581.058
176870	-145.666	-110.522	-4.31581	393.436
176870	-139.421	-104.214	-4.62263	393.436
11511120	-127.929	-100.121	-2.0006	469.939
123631	-131.007	-98.9755	-3.45071	446.902
60953	-130.411	-98.9504	-6.47584	359.35
10297043	-126.492	-97.9906	-2.30242	440.583
3081361	-143.034	-96.9528	-2.74	475.354
3081361	-129.968	-96.8904	-2.40655	475.354
442972	-121.699	-96.8892	-1.69628	411.62
176870	-141.357	-96.4829	-2.04013	393.436

2.2 Virtual screened results

Virtual screening uses high-performance computation to screen vast chemical libraries for potent lead compounds. For the chemical Lapatinib, an advanced similarity search yielded 407 results. The top 10 docking results of the full 407 virtual screened compounds are shown in [Table 3]. The molecule PubChem ID: 59671768, SCHEMBL1427033 is shown in [Fig. 2(II)] as a high-affinity compound with the lowest re-rank score. This molecule has a molecular weight of 581.058 g/mol, a topological surface area of 116A^2, and a logP value of 6.1. It has two hydrogen bond donors and ten hydrogen bond acceptors. Among these 407 compounds, the medication with PubChem CID: 59671768 has a lot of potential as a Glioblastoma inhibitor over the EGFR target protein.

Table 3
Molecular Docking results of virtual screened compounds.

Ligand PubChem ID	MolDock Score	Rerank Score	HBond	MW
59671768	-198.554	-137.713	-3.60625	581.058
118717618	-209.355	-136.801	-8.206	667.147
73713599	-189.563	-134.892	-3.6824	645.143
22017830	-170.591	-134.607	0	609.068
51002442	-179.238	-134.565	-5.44535	581.058
68178766	-189.388	-133.297	-6.46064	581.058
123656076	-199.356	-132.452	-6.42519	597.1
142038799	-185.028	-132.077	-3.80955	613.144
117807540	-185.92	-131.928	-5.51334	583.073
145585441	-178.826	-131.251	-6.64474	580.05
44532710	-184.249	-130.587	-5.35679	595.084
143782896	-190.146	-130.19	-2.40091	581.124
44199881	-188.898	-130.106	-7.01001	581.058
58729910	-193.099	-129.403	-5.12112	567.031
149028802	-169.044	-129.125	-4.56433	595.084
143924483	-176.155	-129.104	-9.4083	627.083
22017830	-197.361	-128.844	-6.58476	609.068
57347591	-168.052	-127.905	-2.36981	581.058

2.3 Molecular Dynamics Simulation

We have simulated ligand-protein complexes with high affinity and low binding energy for 100 ns to compute the RMSD and RMSF with the targeted protein (PDB ID: 5XWD)[41] [Fig. 3, (I-IV)]. The protein and ligand root mean square deviations, which are commonly employed to measure the scalar distance between the protein (C-alpha backbone) and the ligand throughput trajectory, were utilized to calculate the MD of protein-ligand complexes. According to Fig. 3(I), the protein's root mean square deviation remained steady in the presence of an established ligand (PubChem ID: 208908) at 20 ns, later it has shown the highest variations around 14.35 Å between 20 to 80 ns. But at the end of the simulation, the RMSD was noted with the lowest value of ~ 12 Å, & less fluctuations of stability. RMSF (root mean square fluctuation) analysis is to reveal the flexibility of the movement of the atom while the interaction of the

ligand, graphical representation shown in Fig. 3. Overall average RMSF of established compounds with protein was obtained at 4.5–5.0 Å, observed with high differences, shown in Fig. 3(II). In the presence of a virtual screened ligand with targeted protein (PubChem ID: 59671768), the RMSD of the protein complex was noted a sudden high peak of fluctuations from the beginning to 20 to 25ns. But it was started to stabilize with very less fluctuations value of 7.5 to 10.5 Å during the entire simulation period, shown in Fig. 3 (III). Where, the RMSF graph was investigated with a less fluctuation value relative to the established compound with an average value of 3.0–4.0 Å, given in Fig. 3 (IV).

2.4 Protein-Ligand interaction

Protein-ligand interactions indicated the protein's conformational stability and correlation, which allows for a better understanding of simulations. Thus, the detailed investigation of both established and screened compounds were described below.

Lapatinib (PubChem ID: 208908) – The most effective established compound -

Figure 4 shows the results of post-dynamics protein-ligand interaction studies on Lapatinib with EGFR, which indicates that the residues mainly ARG353, GLU388 (from A Chain), SER95, ASP96, SER93 (from B Chain), and TYR61 (from H Chain) revealed a mixture of H-bond, hydrophobic, Salt & Water bridges interactions during the MD simulation. As a result, it has been discovered that most of the interactions are continuously kept following docking. According to a literature review, Lapatinib (PubChem ID: 208908) is also known as Lapatinib Ditosylate, an orally active drug used to treat solid malignancies such as glioblastoma and breast cancer. It's a dual tyrosine kinase inhibitor that works by blocking both the HER2/neu and epidermal growth factor receptor pathways.

SCHEMBL14272033 (PubChem ID: 59671768) – The effective Virtual Screened compound –

The results of post-dynamics protein-ligand interaction studies on SCHEMBL14272033 with EGFR during MD simulation are shown in Fig. 5. Residues like PHE352, ARG353, LEU363, PRO365, TRP386, GLU388, ASN420 (from A Chain) and SER93, SER93 (from D Chain) have been identified with strong H-bond, hydrophobic, Salt & Water bridges interactions with the ligand, accounting for 75 and 80 percent interaction with the protein residues, respectively. Similarly, the virtually screened molecule found with most of the interactions is continually kept following docking investigations, just as established compounds. We believe that SCHEMBL14272033 (PubChem ID: 59671768) can be repurposed as an anticancer medication to treat glioblastoma and breast cancer based on these findings. As a result, it is possible to recommend it for further screening and optimization using *In-vitro* experiments.

2.5 Ligand property

The properties of established and screened compounds are estimated and compared in terms of RMSD, Gyration, molecular surface area (MolSA), solvent accessible surface area (SASA), and polar surface area (PSA), shown in Fig. 6 & Fig. 7.

RMSD - The RMSD of the ligand varies at first, then gradually approaches stabilization towards the conclusion of the simulation time. In the case of the established ligand, RMSD has been noted with a range between 0.8–2.4 Å with an equilibrium value of approximately 1.6Å [Fig. 6]; whereas the best virtual screened ligand exhibits a range of RMSD values between 1.5–3.0 Å with an equilibrium value of around 3.0Å[Fig. 7].

rGyr - If the body's (ligands) total mass were concentrated, the rGyr (gyration) value is the radial distance to a place with the same moment of inertia as the body's (ligands) true distribution of mass. The ligands' rGyr fluctuates dramatically up to 20 ns simulation and then gradually returns to equilibrium. In the case of the established ligand,rGyrexhibits a range between 6–6.8Å with an equilibrium value of ~ 6.4Å [Fig. 6], while the screened ligand exhibits a range of rGyr values between 7.5–8.5 Å with an equilibrium value of ~ 8.0 Å[Fig. 7].

MolSA - MolSA is a method for surface calculation that uses a 1.4 probe radius. The surface area of a van der Waals is equal to this number. In the case of the established ligand, MolSA remains constant throughout the simulation except at 40–65 ns, noted with a range of 510 to 522 $Å^2$with an equilibrium value of 516.$Å^2$[Fig. 6]; whereas the virtual screened ligand remains constant throughout the simulation except at 80–100 ns, and noted with a range of 568 to 592 $Å^2$with an equilibrium value of 584 $Å^2$[Fig. 7].

SASA - The surface area of a molecule that can be reached by a water molecule is referred to as SASA. The established ligand's SASA is constant and shows no notable fluctuations until gradually nearing equilibrium, but the screened compound showed higher stability practically throughout the simulation, with only a minor fluctuation near the conclusion. The established compound identified the SASA range of 240–420$Å^2$with an equilibrium value of 300$Å^2$[Fig. 6]; whereas the virtual screened ligand exhibits the SASA range of around 300 to 750 $Å^2$with an equilibrium value of approximately 450 $Å^2$[Fig. 7].

PSA -The solvent-accessible surface area of a molecule made solely of oxygen and nitrogen atoms is referred to as PSA. The established ligand exhibits a PSA range of 120–165 $Å^2$ with an equilibrium value of 135$Å^2$[Fig. 6]; whereas the screened compound’s PSA exhibits an early variation of up to 35 ns, which has a PSA range of around 135 to 180 $Å^2$with an equilibrium value of approximately 165$Å^2$[Fig. 7]. Overall, it is concluded that all ligand characteristics gradually stabilize and prove the ligand's stability at the protein's active site.

2.6 Drug - Drug comparison studies

Table 4 displays the re-rank scores of the compounds against the Glioblastoma target protein EGFR. The total energy of the newly discovered inhibitor PubChem ID- 59671768 was the lowest among the complete virtual screened molecules, indicating its higher affinity. Surprisingly, according to the steric energy of PLP (Piecewise Linear Potential), the other interaction of both compound’s displaying the virtual screened compound has less affinity interaction properties than the pre-established Lapatinib. Because the virtual screened compound's hydrogen bond stability is similar to that of the established

inhibitor Lapatinib, which makes the newly screened compound a novel therapeutic for EGFR in Glioblastoma.

Table 4
The Drug-Drug comparison studies between established and screened compounds.

	Established Compound PubChem ID:208908		Virtual Screened Compound PubChem ID: 59671768	
Energy overview Descriptors	**MolDock Score**	**Rerank Score**	**MolDock Score**	**Rerank Score**
Total Energy	-154.117	-115.565	-198.554	-137.713
External Ligand interactions	-187.094	-155.135	-220.187	-184.185
Protein - Ligand interactions	-187.094	-155.135	-220.187	-184.185
Steric (by PLP)	-180.583	-123.88	-218.025	-149.565
Hydrogen bonds	-6.511	-5.156	-4.162	-3.712
Internal Ligand interactions	32.977	39.57	43.472	44.473
Torsional strain	16.463	15.442	18.632	17.477
Hydrogen bonds		0		0
Steric (by PLP)	16.514	2.84	24.84	4.273

2.8 Pharmacophore mapping images

Pharmacophore mapping, in addition to molecular docking, provides a three-dimensional basic systemic topography of molecular interaction with complicated target receptors. Pharmacophore studies introduce a specific phenomenon about the best interaction mode for a certain target annotation and describe the molecule's aligned poses, which helps us figure out how the target protein and the novel drug interact. Even with Lapatinib's excellent affinity and good interaction profile (PubChem ID: 208908) shows hydrogen bonding between the drug and residues LYS31, GLU388, TYR3 [Fig. 8(A)]. The interaction of the practically screened chemical compound SCHEMBL14272033 (PubChem ID: 59671768) with the cavity of the target protein EGFR reveals that the residues ASN27, ASN420, TRP386 found with hydrogen bonding with ligands [Fig. 8(B)].

2.9 ADME/T studies

Table 5 displays the estimated ADME/T value for the best virtual screened compound (PubChem CID: 59671768) and established inhibitor (PubChem CID: 208908). A virtual screened compound has a greater absorptive value than an established compound in every way; the established compound's BBB + value is 0.9738, while the virtually screened molecule's value is 0.9755. The bioavailability indication for the two top docking findings derived from the SwissADME online tool demonstrates the compounds' activity potential. The established molecule has a higher P-glycoprotein probability value than the virtually

screened compound, implying that it is more lipophilic. Both chemicals can be present in the cell, although in distinct places. Although the practically screened compound (PubChem CID: 59671768) exhibits high CYP inhibitor promiscuity and might be employed as a CYP3A4 inducer inhibitor, and other way it has a lower possibility of acting as a substrate for CYP450 2C9 and CYP450 2D6 than the established chemical. AMES toxicity is absent in both compounds, demonstrating that they are not mutagenic. The regression value for absorption and toxicity (in terms of aqueous solubility and rat acute toxicity of parecoxib) has been noted with a higher value in the established compounds than in virtual screening compounds, shown in Table 6. R programming was used to create a graphical depiction of the comparative research between the two best virtual screened substances and the two best-established compounds [Fig. 9]. It demonstrates that the virtual screening chemical (PubChem CID 59671768) is significantly less toxic than the established drug (PubChem CID 208908), and that its absorption and BBB values are comparable to the established compound.

Table 5
ADME/T profile studies performed with admetSAR tool.

ADMET predicted profile	Virtual Screened Compound PubChem ID: 59671768		Established Compound PubChem ID:208908	
	Value	Probability	Value	Probability
Human Intestinal Absorption	+	0.9774	+	0.9814
Caco-2	-	0.8460	-	0.8511
Blood Brain Barrier	+	0.9755	+	0.9738
Human oral bioavailability	-	0.5827	-	0.8429
Subcellular localzation	Mitochondria	0.3474	Lysosomes	0.4124
OATP2B1 inhibitior	+	0.7163	+	0.5751
OATP1B1 inhibitior	+	0.8420	+	0.8609
OATP1B3 inhibitior	+	0.9394	+	0.9386
MATE1 inhibitior	-	0.7400	-	0.7200
OCT2 inhibitior	+	0.5750	-	0.5500
BSEP inhibitior	+	0.9882	+	0.9971
P-glycoprotein inhibitior	+	0.8933	+	0.8639
P-glycoprotein substrate	+	0.8717	+	0.9343
CYP3A4 substrate	+	0.7109	+	0.6943
CYP2C9 substrate	-	0.8087	-	1.0000
CYP2D6 substrate	-	0.7664	-	0.7463
CYP3A4 inhibition	+	0.8224	+	0.8065
CYP2C9 inhibition	+	0.5000	-	0.5544
CYP2C19 inhibition	+	0.6282	+	0.5274
CYP2D6 inhibition	-	0.7210	-	0.7861
CYP1A2 inhibition	+	0.6637	+	0.5386
CYP inhibitory promiscuity	+	0.8989	+	0.9104
UGT catelyzed	-	0.0000	-	0.0000
Carcinogenicity (binary)	-	0.9286	-	0.9286
Carcinogenicity (trinary)	Non-required	0.5442	Non-required	0.5703

ADMET predicted profile	Virtual Screened Compound PubChem ID: 59671768		Established Compound PubChem ID:208908	
	Value	Probability	Value	Probability
Eye corrosion	-	0.9836	-	0.9886
Eye irritation	-	0.9531	-	0.9541
Ames mutagenesis	-	0.5700	-	0.5400
Human either-a-go-go inhibition	+	0.9488	+	0.9566
micronuclear	+	0.8700	+	0.9100
Hepatotoxicity	+	0.6000	+	0.7250
Acute Oral Toxicity (c)	III	0.5778	III	0.5949
Estrogen receptor binding	+	0.8483	+	0.8218
Androgen receptor binding	+	0.8934	+	0.8909
Thyroid receptor binding	+	0.6652	+	0.6466
Glucocorticoid receptor binding	+	0.7627	+	0.6743
Aromatase binding	+	0.5838	+	0.5872
PPAR gamma	+	0.7981	+	0.7119
Honey bee toxicity	-	0.7272	-	0.7526
Biodegradation	-	0.9000	-	0.8250
crustacea aquatic toxicity	+	0.6800	+	0.6200
Fish aquatic toxicity	+	0.6826	+	0.9246

Table 6
ADMET predicted profile – Regressions.

	Virtual Screened Compound PubChem ID: 59671768		Established Compound PubChem ID:208908	
	Value	Unit	Value	Unit
Water solubility	-3.501	logS	-3.647	logS
Plasma protein binding	1.245	100%	1.201	100%
Acute Oral Toxicity	2.894	kg/mol	3.089	kg/mol
Tetrahymena pyriformis	1.89	pIGC50 (ug/L)	1.124	pIGC50 (ug/L)

2.10 Boiled egg Plot

The Boiled Egg plot attempts to forecast the drugs' gastrointestinal absorption and blood-brain barrier characteristics. For the same objective, the best pre-established inhibitor lapatinib (PubChem ID: 208908, PubChem ID: 176870) and the best virtual screening inhibitors (Pub CID: 59671768, Pub ID: 118717618) were chosen. [Fig. 10]. The virtual screened compounds (Pub CID: 59671768, Pub ID: 118717618) are present in the yolk region of the egg plot, indicating that the virtually screened compound is capable of crossing the blood-brain barrier, which is required for the treatment of glioblastoma. When compared to the best-established compounds, both are present in the grey region, indicating their lower gastrointestinal absorption and inability to cross the blood-brain barrier.

The Bioavailability Radar efficiently analyzes a molecule's drug-likeness. Each property has a pink area that represents the optimal range (lipophilicity: XLOGP3 between 0.7 and + 5.0, size: MW between 150 and 500 g/mol, polarity: TPSA between 20 and 1302, solubility: logS significantly less than 6, saturation: percentage of carbons in the sp3 hybridization not more than 25%, and flexibility: no more than 9 rotatable bonds). Figure 11 depicts the bioavailability map for both well-established and virtually screened substances.

3. Material And Methods

Schrodinger's Drug Discovery Suite (Schrodinger, Inc., LLC, New York, USA) [42–46] Molegro Virtual Docker[47–53], and admetSAR webserver are used in this study[54–57]. Desmond, Schrodinger was used to run the entire simulation and related research. PyMol, Schrodinger, MS-Excel, and R-Programming were used to make the visualization images [58–62].

3.1 Selection of inhibitors

Current EGFR inhibitors targeting GBM were identified by a survey of the literature to begin the collection of inhibitors. A total of 16 recognized inhibitors were available for further investigation. The three-dimensional structures of certain inhibitors were missing. The three-dimensional structures of all of those chemicals were modeled in Marvin Sketch and saved in a three-dimensional SDF file[63–67]. Below, Table.1 represents all 16 inhibitors along with their PubChem IDs [68–74].

3.2 Protein and ligand preparation

The crystal structure of the target protein, an extracellular region of EGFR, was obtained from the Protein Data Bank (PDB) under accession number PDB ID: 5XWD [41] for molecular docking studies. Download crystal coordinates of protein were prepared using Protein Preparation Wizard, Schrödinger Software by keeping default parameters of assigning bond orders, optimizing and minimization using OPLS_2005 with root mean square deviation (RMSD) value of 0.30 Å [42–46]. All the collected compounds from PubChem Database were taken into the platform of the LigPrep module, Schrödinger, which was prepared

for proper conversion of 2D to 3D, neutralization of charge, stereoisomer generation, and ionization state at pH value 7.2 ± 0.2 by applying force field OPLS-2005[75–81].

3.3 Molecular docking

The Molegro Virtual Docker (MVD), which is integrated with the high-potential Piece Wise Linear Potential (PLP) and the MVD scoring tool [82–84], was used to conduct the docking study. A single SDF format was used to save the 16 ligands that had been planned ahead of time. The target protein's PDB file was deleted since it already has ligands. After that, it was prepared further by detecting cavities. For subsequent docking with ligands method, a cavity was chosen, specifically the third cavity with a volume of 94.72A^{o}. The protein and ligands were tested for binding affinity using the following conformations: internal electrostatic interaction (Internal ES), sp2-sp2 torsions, and internal hydrogen bond interaction; in which, the docking procedure was set with a median iteration of 1,500, a maximum population size of 50, and a grid solution of 0.2[85–88]. The binding site determined the first cavity based on the highest volume. The post-dock analysis had two goals: energy minimization and H-bond optimization. After docking, the Nelder Mead Simplex Minimization (using a non-grid force field and H-bond directionality) was employed to reduce the ligand-receptor interaction's dynamic energy[89–93].

3.4 High throughput virtual screening

A similarity search was run against the PubChem database developed by the National Institutes of Health, which is one of the public chemical repositories comprising around 93 million chemical compounds, in relation to our query compound Laptinib[89][91]. The NCBI's PubChem compound database was filtered using the component rule of Lipinski's rule of five at a threshold of > = 95 percent [87–91]. These compounds were all put through the same process, which comprised Molecular Docking with the target protein EGFR to find the chemical with the best affinity[92–93].

3.5 Molecular Dynamics Simulation

Molecular dynamics simulations on the two compounds that showed low binding energy ligand-protein complexes during docking were performed using the Desmond Simulation Software, Schrodinger[94–97]. Individually, all the complexes were solvated in an explicit water box of size 10 with periodic boundary conditions (PBC) using a water model TIP3P. Then, the complexes were simulated using the OPLS3e force field and Na^{+} and Cl^{-}ions were added to make the system's overall charge neutral. Following that, the prepared system was subjected to a 2000-step energy minimization before being put through a 100-ns production run[98–101]. Further, all the systems were taken into MDS for 100 ns with default relaxation protocol followed by periodic boundary conditions with a number of atoms, pressure, and temperature (NPT) ensemble, where, temperature Nose-Hoover and isotropic scaling were utilized to adjust the temperature at 300K and atmospheric pressure at 1atm. Later, complete results were analyzed by monitoring the RMSD and RMSF using the Simulation Interaction Diagram tool in the Desmond package [102–106].

3.6 Drug -Drug comparative studies

The unidentified complex structure was discovered using the existing drug docking result. It was cleared by removing all ligands, constraints, and cavities except the protein, which was then imported with the best-posed inhibitor and exported as an SDF file with the best drug docked file[89]. After obtaining the complicated structure from the virtual docking result, the procedure was repeated. In order to select the optimal inhibitor, the excel sheet was utilized to compare all of the affinities, hydrogen interactions, steric energy, and lowest re-rank score [57–59].

3.7 ADMET studies

The non-commercial admetSAR database provides a query interface for a unique biological and chemical profile[107]. The ADME/T profile includes qualities such as adsorption, digestion, metabolism, excretion, and toxicity, all of which are important in the development and discovery of drugs. The database ideally includes five quantitative regression models and 22 qualitative classifications, yielding a highly predictive result. The properties of the database were calculated with the help of admetSAR[59–62].

3.8 Boiled Egg Plot

The boiled egg (Brain or Intestinal Estimated permeation method) plot is a reliable indicator of small molecule lipophilicity and polarity. It includes a statistical plot that forecasts two essential passive predictions, gastrointestinal absorption and brain penetration, both of which are important pharmacokinetic parameters for the creation of a new drug. Molecular weight, TPSA, MLOGP, GI, and BBB are some of the other properties [89]. The boiled egg plot is a three-region cartesian plan with yellow (yolk area), white, and grey. As a result, if the chemical of interest is in the yolk region, the possibility of a Blood-Brain Barrier is increased, but if it is in the white region, the likelihood of great intestinal absorption increases. If the molecule of relevance is in the grey zone, it is more likely to be non-absorptive and non-penetrative. This is achieved through SwissADME is a software that evaluates substances for ADME, physicochemical properties, drug-likeness, and pharmacokinetics. The Marvin JS molecular sketcher from ChemAxon (http://www.chemaxon.com) is incorporated into the input zone, allowing users to import (from a file or an external database), sketch, and edit 2D chemical structure diagrams before transferring them to a list of molecules [57–59]. This list, which is located on the right of the submission page, serves as the input for calculation. SMILES can be input or copied in the same way that regular text is. In the list, an input molecule is identified by a SMILES and, optionally, a name separated by spaces [89].

Discussion

Glioblastoma, being the most severe clinical condition, piqued the interest of scientists and researchers all over the world. Despite having several glioblastoma treatments, including chemotherapy, radiation therapy, and surgery, the literature suggests that diagnosed patients may not have a high chance of long-term survival and may experience a variety of adverse effects [96]. We presented a novel inhibitor capable of directly blocking the EGFR active site in the current study. Lapatinib PubChem CID: 208908 was discovered to be the most well-known of the 16 developed EGFR inhibitors for the treatment of glioblastoma.

Conclusion

As the incidence of glioblastoma has increased, so it has the scope of pharmaceutical research. Analgesics to target certain drugs are being developed swiftly as EGFR selective inhibitors for glioblastoma therapy. The goal of this research is to show that a novel inhibitor discovered through virtual screening is effective against the drug target. This small chemical has a higher affinity for the target EGFR protein receptor. Among the 14 pre-established drugs found through literature searches, lapatinib was shown to be the most effective one. Virtual screening and docking studies were performed on this compound in order to find the most effective chemical PubChem CID: 59671768. Comparative studies show that the virtual screened molecule has a higher EGFR receptor affinity score and binding capability. The pharmacophore mapping of this molecule shows that it interacts optimally with the receptor protein, which supports findings from molecular dynamic simulation.

Furthermore, the compound (PubChem CID: 59671768) noted with non-toxic and non-carcinogenic, with gastrointestinal absorption and BBB probability that is comparable to present compounds based on the ADME/T study. The bioavailability and toxicity of this virtually tested compound are major to be higher. *In-vitro* testing is also required to assess its pharmacokinetic and pharmacodynamic properties, therapeutic value in the treatment of glioblastoma, and overall efficacy in comparison to other drugs.

Declarations

AUTHOR CONTRIBUTIONS

AP contributed equally to this work with MA. AP, MA and was involved in Molecular docking, Molecular Dynamics Simulation, Writing – review & editing. MM, IC, AB, LS, NV, UP, LP, DG, and PB were contributed to Inhibitors collection, Data curation, Formal analysis, Validation, and Visualization. AP and MA were involved in Molecular dynamic simulation. SA, TH, IC, MAK, CS and LS were also involved in Molecular Docking, ADMET analysis, R Programming analysis, and Writing – review & editing. SA, TH, AN, and SKS were contributed to the investigation, supervision, writing – review & editing

Conflicts of interest/Competing interests:

The authors declare that they have no conflict of interest.

AVAILABILITY OF DATA AND MATERIALS:

Not applicable.

Code Availability:

Code will be provided as per the request

ETHICS APPROVAL AND CONSENT TO PARTICIPATE:

Not applicable.

HUMAN AND ANIMAL RIGHTS:

No animals/humans were used in the studies that are the basis of this research.

Acknowledgements:

1. We thank Taif University Researchers Supporting Project Number (TURSP-2020/202), Taif University, Taif, Saudi Arabia
2. The authors are grateful to the Deanship of Scientific Research, King Saud University for funding through Vice Deanship of Scientific Research Chairs.
3. SKS thank Alagappa University, Department of Biotechnology (DBT), New Delhi (No. BT/PR8138/BID/7/458/2013, dated 23rd May 2013), DST-PURSE 2nd Phase Programme Order No. SR/PURSE Phase 2/38 (G dated 21.02.2017 and FIST (SR/FST/LSI - 667/2016), MHRD RUSA 1.0 and RUSA 2.0 for providing the financial assistance. UP gratefully acknowledge Indian Council of Medical Research (ISRM/11/ (19)/2017, dated: 09.08.2018).

Conflict of Interest:

The Author(s) declare that there is no conflict of interest.

References

1. Karsy, M., Huang, T., Kleinman, G. and Karpel-Massler, G., 2014. Molecular, histopathological, and genomic variants of glioblastoma. Frontiers in bioscience (Landmark edition), 19, p.1065.
2. Kita, D., Yonekawa, Y., Weller, M. and Ohgaki, H., 2007. PIK3CA alterations in primary (de novo) and secondary glioblastomas. Acta neuropathologica, 113(3), pp.295-302.
3. Philip, R., Carrington, L. and Chan, M., 2011. US FDA perspective on challenges in co-developing in vitro companion diagnostics and targeted cancer therapeutics. Bioanalysis, 3(4), pp.383-389.
4. Phillips, J.J., Aranda, D., Ellison, D.W., Judkins, A.R., Croul, S.E., Brat, D.J., Ligon, K.L., Horbinski, C., Venneti, S., Zadeh, G. and Santi, M., 2013. PDGFRA Amplification is Common in Pediatric and Adult High-Grade Astrocytomas and Identifies a Poor Prognostic Group in IDH 1 Mutant Glioblastoma. Brain pathology, 23(5), pp.565-573.
5. Rich, J.N., Hans, C., Jones, B., Iversen, E.S., McLendon, R.E., Rasheed, B.A., Dobra, A., Dressman, H.K., Bigner, D.D., Nevins, J.R. and West, M., 2005. Gene expression profiling and genetic markers in glioblastoma survival. Cancer research, 65(10), pp.4051-4058.
6. Wong, A.J., Ruppert, J.M., Bigner, S.H., Grzeschik, C.H., Humphrey, P.A., Bigner, D.S. and Vogelstein, B., 1992. Structural alterations of the epidermal growth factor receptor gene in human gliomas. Proceedings of the National Academy of Sciences, 89(7), pp.2965-2969.

7. Salkeni, M.A., Zarzour, A., Ansay, T.Y., McPherson, C.M., Warnick, R.E., Rixe, O. and Bahassi, E.M., 2013. Detection of EGFRvIII mutant DNA in the peripheral blood of brain tumor patients. Journal of neuro-oncology, 115(1), pp.27-35.
8. Labussière, M., Boisselier, B., Mokhtari, K., Di Stefano, A.L., Rahimian, A., Rossetto, M., Ciccarino, P., Saulnier, O., Paterra, R., Marie, Y. and Finocchiaro, G., 2014. Combined analysis of TERT, EGFR, and IDH status defines distinct prognostic glioblastoma classes. Neurology, 83(13), pp.1200-1206.
9. Krell, D., Mulholland, P., Frampton, A.E., Krell, J., Stebbing, J. and Bardella, C., 2013. IDH mutations in tumorigenesis and their potential role as novel therapeutic targets. Future oncology, 9(12), pp.1923-1935.
10. Weller, M., Kaulich, K., Hentschel, B., Felsberg, J., Gramatzki, D., Pietsch, T., Simon, M., Westphal, M., Schackert, G., Tonn, J.C. and von Deimling, A., 2014. Assessment and prognostic significance of the epidermal growth factor receptor vIII mutation in glioblastoma patients treated with concurrent and adjuvant temozolomide radiochemotherapy. International journal of cancer, 134(10), pp.2437-2447.
11. Wemmert, S., Ketter, R., Rahnenfuhrer, J., Beerenwinkel, N., Strowitzki, M., Feiden, W., Hartmann, C., Lengauer, T., Stockhammer, F., Zang, K.D. and Meese, E., 2005. Patients with high-grade gliomas harboring deletions of chromosomes 9p and 10q benefit from temozolomide treatment. Neoplasia, 7(10), pp.883-893.
12. E Taylor, T., B Furnari, F. and K Cavenee, W., 2012. Targeting EGFR for treatment of glioblastoma: molecular basis to overcome resistance. Current cancer drug targets, 12(3), pp.197-209.
13. Zhao, J., Ma, W. and Zhao, H., 2014. Loss of heterozygosity 1p/19q and survival in glioma: a meta-analysis. Neuro-oncology, 16(1), pp.103-112.
14. Herbst, R.S., 2004. Review of epidermal growth factor receptor biology. International Journal of Radiation Oncology* Biology* Physics, 59(2), pp.S21-S26.
15. Opresko, L.K., Chang, C.P., Will, B.H., Burke, P.M., Gill, G.N. and Wiley, H.S., 1995. Endocytosis and lysosomal targeting of epidermal growth factor receptors are mediated by distinct sequences independent of the tyrosine kinase domain. Journal of Biological Chemistry, 270(9), pp.4325-4333.
16. Chistiakov, D.A., Chekhonin, I.V. and Chekhonin, V.P., 2017. The EGFR variant III mutant as a target for immunotherapy of glioblastoma multiforme. European journal of pharmacology, 810, pp.70-82.
17. Spivak-Kroizman, T., Rotin, D., Pinchasi, D., Ullrich, A., Schlessinger, J. and Lax, I., 1992. Heterodimerization of c-erbB2 with different epidermal growth factor receptor mutants elicits stimulatory or inhibitory responses. Journal of Biological Chemistry, 267(12), pp.8056-8063.
18. Downward, J., Parker, P. and Waterfield, M.D., 1984. Autophosphorylation sites on the epidermal growth factor receptor. Nature, 311(5985), pp.483-485.
19. Singh, A.B. and Harris, R.C., 2005. Autocrine, paracrine and juxtacrine signaling by EGFR ligands. Cellular signalling, 17(10), pp.1183-1193.
20. Lo, H.W., Cao, X., Zhu, H. and Ali-Osman, F., 2008. Constitutively activated STAT3 frequently coexpresses with epidermal growth factor receptor in high-grade gliomas and targeting STAT3 sensitizes them to Iressa and alkylators. Clinical cancer research, 14(19), pp.6042-6054.

21. Zheng, Q., Han, L., Dong, Y., Tian, J., Huang, W., Liu, Z., Jia, X., Jiang, T., Zhang, J., Li, X. and Kang, C., 2014. JAK2/STAT3 targeted therapy suppresses tumor invasion via disruption of the EGFRvIII/JAK2/STAT3 axis and associated focal adhesion in EGFRvIII-expressing glioblastoma. Neuro-oncology, 16(9), pp.1229-1243.
22. Lo, H.W., Cao, X., Zhu, H. and Ali-Osman, F., 2010. Cyclooxygenase-2 is a novel transcriptional target of the nuclear EGFR-STAT3 and EGFRvIII-STAT3 signaling axes. Molecular Cancer Research, 8(2), pp.232-245.
23. la Iglesia, N.D., Puram, S.V. and Bonni, A., 2009. STAT3 regulation of glioblastoma pathogenesis. Current molecular medicine, 9(5), pp.580-590.
24. De La Iglesia, N., Konopka, G., Lim, K.L., Nutt, C.L., Bromberg, J.F., Frank, D.A., Mischel, P.S., Louis, D.N. and Bonni, A., 2008. Deregulation of a STAT3–interleukin 8 signaling pathway promotes human glioblastoma cell proliferation and invasiveness. Journal of Neuroscience, 28(23), pp.5870-5878.
25. Del Vecchio, C.A., Jensen, K.C., Nitta, R.T., Shain, A.H., Giacomini, C.P. and Wong, A.J., 2012. Epidermal growth factor receptor variant III contributes to cancer stem cell phenotypes in invasive breast carcinoma. Cancer research, 72(10), pp.2657-2671.
26. Zhou, J., Yi, L., Ouyang, Q., Xu, L., Cui, H. and Xu, M., 2014. Neurotensin signaling regulates stem-like traits of glioblastoma stem cells through activation of IL-8/CXCR1/STAT3 pathway. Cellular signalling, 26(12), pp.2896-2902.
27. Eyler, C.E., Wu, Q., Yan, K., MacSwords, J.M., Chandler-Militello, D., Misuraca, K.L., Lathia, J.D., Forrester, M.T., Lee, J., Stamler, J.S. and Goldman, S.A., 2011. Glioma stem cell proliferation and tumor growth are promoted by nitric oxide synthase-2. Cell, 146(1), pp.53-66.
28. Charles, N., Ozawa, T., Squatrito, M., Bleau, A.M., Brennan, C.W., Hambardzumyan, D. and Holland, E.C., 2010. Perivascular nitric oxide activates notch signaling and promotes stem-like character in PDGF-induced glioma cells. Cell stem cell, 6(2), pp.141-152.
29. Lo, H.W., Cao, X., Zhu, H. and Ali-Osman, F., 2010. Cyclooxygenase-2 is a novel transcriptional target of the nuclear EGFR-STAT3 and EGFRvIII-STAT3 signaling axes. Molecular Cancer Research, 8(2), pp.232-245.
30. Greenhough, A., Smartt, H.J., Moore, A.E., Roberts, H.R., Williams, A.C., Paraskeva, C. and Kaidi, A., 2009. The COX-2/PGE 2 pathway: key roles in the hallmarks of cancer and adaptation to the tumour microenvironment. Carcinogenesis, 30(3), pp.377-386.
31. Lo, H.W., Hsu, S.C., Xia, W., Cao, X., Shih, J.Y., Wei, Y., Abbruzzese, J.L., Hortobagyi, G.N. and Hung, M.C., 2007. Epidermal growth factor receptor cooperates with signal transducer and activator of transcription 3 to induce epithelial-mesenchymal transition in cancer cells via up-regulation of TWIST gene expression. Cancer research, 67(19), pp.9066-9076.
32. Lo, H.W., Cao, X., Zhu, H. and Ali-Osman, F., 2008. Constitutively activated STAT3 frequently coexpresses with epidermal growth factor receptor in high-grade gliomas and targeting STAT3 sensitizes them to Iressa and alkylators. Clinical cancer research, 14(19), pp.6042-6054.

33. Kang, S.H., Yu, M.O., Park, K.J., Chi, S.G., Park, D.H. and Chung, Y.G., 2010. Activated STAT3 regulates hypoxia-induced angiogenesis and cell migration in human glioblastoma. Neurosurgery, 67(5), pp.1386-1395.
34. Yiin, J.J., Hu, B., Schornack, P.A., Sengar, R.S., Liu, K.W., Feng, H., Lieberman, F.S., Chiou, S.H., Sarkaria, J.N., Wiener, E.C. and Ma, H.I., 2010. ZD6474, a multitargeted inhibitor for receptor tyrosine kinases, suppresses growth of gliomas expressing an epidermal growth factor receptor mutant, EGFRvIII, in the brain. Molecular cancer therapeutics, 9(4), pp.929-941.
35. Hu, J., Jo, M., Cavenee, W.K., Furnari, F., VandenBerg, S.R. and Gonias, S.L., 2011. Crosstalk between the urokinase-type plasminogen activator receptor and EGF receptor variant III supports survival and growth of glioblastoma cells. Proceedings of the National Academy of Sciences, 108(38), pp.15984-15989.
36. Kotipatruni, R.R., Nalla, A.K., Asuthkar, S., Gondi, C.S., Dinh, D.H. and Rao, J.S., 2012. Apoptosis induced by knockdown of uPAR and MMP-9 is mediated by inactivation of EGFR/STAT3 signaling in medulloblastoma. PloS one, 7(9), p.e44798.
37. Cao, X., Zhu, H., Ali-Osman, F. and Lo, H.W., 2011. EGFR and EGFRvIII undergo stress-and EGFR kinase inhibitor-induced mitochondrial translocalization: a potential mechanism of EGFR-driven antagonism of apoptosis. Molecular cancer, 10(1), pp.1-13.
38. Chumbalkar, V., Latha, K., Hwang, Y., Maywald, R., Hawley, L., Sawaya, R., Diao, L., Baggerly, K., Cavenee, W.K., Furnari, F.B. and Bogler, O., 2011. Analysis of phosphotyrosine signaling in glioblastoma identifies STAT5 as a novel downstream target of ΔEGFR. Journal of proteome research, 10(3), pp.1343-1352.
39. Huang, H.J.S., Nagane, M., Klingbeil, C.K., Lin, H., Nishikawa, R., Ji, X.D., Huang, C.M., Gill, G.N., Wiley, H.S. and Cavenee, W.K., 1997. The enhanced tumorigenic activity of a mutant epidermal growth factor receptor common in human cancers is mediated by threshold levels of constitutive tyrosine phosphorylation and unattenuated signaling. Journal of Biological Chemistry, 272(5), pp.2927-2935.
40. Fan, Q.W., Cheng, C.K., Gustafson, W.C., Charron, E., Zipper, P., Wong, R.A., Chen, J., Lau, J., Knobbe-Thomsen, C., Weller, M. and Jura, N., 2013. EGFR phosphorylates tumor-derivedEGFRvIII driving STAT3/5 and progression in glioblastoma. Cancer cell, 24(4), pp.438-449.
41. Matsuda, T., Ito, T., Takemoto, C., Katsura, K., Ikeda, M., Wakiyama, M., Kukimoto-Niino, M., Yokoyama, S., Kurosawa, Y. and Shirouzu, M. (2018). Cell-free synthesis of functional antibody fragments to provide a structural basis for antibody–antigen interaction. PloS one, 13(2), e0193158.
42. Schrodinger, LLC, NY, USA, 2009
43. LigPrep, Schrodinger LLC, Ney York, NY.
44. Prime, Schrodinger, LLC, Ney York, NY.
45. Protein Preparation Wizard, Schrodinger, LLC, Ney York, NY.
46. Qikprop, Schrodinger, LLC, Ney York, NY.
47. Bitencourt-Ferreira, G., & Azevedo, W. F. D. (2019). Molegro virtual docker for docking. In Docking screens for drug discovery (pp. 149-167). Humana, New York, NY.

48. Adhikary, R., Khandelwal, R., Hussain, T., Nayarisseri, A., & Singh, S. K. (2021). Structural insights into the molecular design of ros1 inhibitor for the treatment of non-small cell lung cancer (nsclc). Current Computer-Aided Drug Design, 17(3), 387-401.
49. Aher, A., Udhwani, T., Khandelwal, R., Limaye, A., Hussain, T., Nayarisseri, A., & Singh, S. K. (2020). In silico insights on IL-6: A potential target for multicentric castleman disease. Current computer-aided drug design, 16(5), 641-653.
50. Ali, M. A., Vuree, S., Goud, H., Hussain, T., Nayarisseri, A., & Singh, S. K. (2019). Identification of high-affinity small molecules targeting gamma secretase for the treatment of Alzheimer's disease. Current topics in medicinal chemistry, 19(13), 1173-1187.
51. Bandaru, S., Alvala, M., Akka, J., Sagurthi, S. R., Nayarisseri, A., Kumar Singh, S., & Prasad Mundluru, H. (2016). Identification of small molecule as a high affinity β2 agonist promiscuously targeting wild and mutated (Thr164Ile) β 2 adrenergic receptor in the treatment of bronchial asthma. Current pharmaceutical design, 22(34), 5221-5233.
52. Bandaru, S., GangadharanSumithnath, T., Sharda, S., Lakhotia, S., Sharma, A., Jain, A., Hussain, T., Nayarisseri, A. and Kumar Singh, S. (2017). Helix-Coil transition signatures B-Raf V600E mutation and virtual screening for inhibitors directed against mutant B-Raf. Current drug metabolism, 18(6), 527-534.
53. Bandaru, S., Tiwari, G., Akka, J., Kumar Marri, V., Alvala, M., Ravi Gutlapalli, V.,& Prasad Mundluru, H. (2015). Identification of high affinity bioactive Salbutamol conformer directed against mutated (Thr164Ile) beta 2 adrenergic receptor. Current topics in medicinal chemistry, 15(1), 50-56.
54. Gudala, S., Khan, U., Kanungo, N., Bandaru, S., Hussain, T., Parihar, M. S., & Mundluru, H. P. (2016). Identification and pharmacological analysis of high efficacy small molecule inhibitors of EGF-EGFR interactions in clinical treatment of non-small cell lung carcinoma: A computational approach. Asian Pacific Journal of Cancer Prevention, 16(18), 8191-8196.
55. Gutlapalli, V. R., Sykam, A., Nayarisseri, A., Suneetha, S., & Suneetha, L. M. (2015). Insights from the predicted epitope similarity between Mycobacterium tuberculosis virulent factors and its human homologs. Bioinformation, 11(12), 517.
56. Jain, D., Udhwani, T., Sharma, S., Gandhe, A., Reddy, P. B., Nayarisseri, A., & Singh, S. K. (2019). Design of novel JAK3 Inhibitors towards Rheumatoid Arthritis using molecular docking analysis. Bioinformation, 15(2), 68.
57. Khandelwal, R., Chauhan, A.P., Bilawat, S., Gandhe, A., Hussain, T., Hood, E.A., Nayarisseri, A. and Singh, S.K. (2018). Structure-based virtual screening for the identification of high-affinity small molecule towards STAT3 for the clinical treatment of osteosarcoma. Current topics in medicinal chemistry, 18(29), 2511-2526.
58. Limaye, A., Sweta, J., Madhavi, M., Mudgal, U., Mukherjee, S., Sharma, S., Hussain, T., Nayarisseri, A. and Singh, S.K. (2019). In silico insights on gd2: a potential target for pediatric neuroblastoma. Current topics in medicinal chemistry, 19(30), 2766-2781.

59. Majhi, M., Ali, M. A., Limaye, A., Sinha, K., Bairagi, P., Chouksey, M., & Singh, S. K. (2018). An in silico investigation of potential EGFR inhibitors for the clinical treatment of colorectal cancer. Current topics in medicinal chemistry, 18(27), 2355-2366.
60. Qureshi, S., Khandelwal, R., Madhavi, M., Khurana, N., Gupta, N., Choudhary, S.K., Suresh, R.A., Hazarika, L., Srija, C.D., Sharma, K. and Hindala, M.R., (2021). A Multi-Target Drug Designing for BTK, MMP9, Proteasome And TAK1 for the clinical treatment of Mantle Cell Lymphoma. Curr Top Med Chem. 21(9):790-818.
61. Shukla, P., Khandelwal, R., Sharma, D., Dhar, A., Nayarisseri, A., & Singh, S. K. (2019). Virtual screening of IL-6 inhibitors for idiopathic arthritis. Bioinformation, 15(2), 121.
62. Sinha, K., Majhi, M., Thakur, G., Patidar, K., Sweta, J., Hussain, T., Nayarisseri, A. and Singh, S.K. (2018). Computer-aided drug designing for the identification of high-affinity small molecule targeting cd20 for the clinical treatment of chronic lymphocytic leukemia (CLL). Current topics in medicinal chemistry, 18(29), 2527-2542.
63. Sweta, J., Khandelwal, R., Srinitha, S., Pancholi, R., Adhikary, R., Ali, M.A., Nayarisseri, A., Vuree, S. and Singh, S.K. (2019). Identification of high-affinity small molecule targeting IDH2 for the clinical treatment of acute myeloid leukemia. Asian Pacific Journal of Cancer Prevention: APJCP, 20(8), 2287.
64. Nayarisseri, A., Moghni, S. M., Yadav, M., Kharate, J., Sharma, P., Chandok, K. H., & Shah, K. P. (2013). In silico investigations on HSP90 and its inhibition for the therapeutic prevention of breast cancer. journal of pharmacy research, 7(2), 150-156.
65. Nayarisseri, A., Yadav, M., & Wishard, R. (2013). Computational evaluation of new homologous down regulators of Translationally Controlled Tumor Protein (TCTP) targeted for tumor reversion. Interdisciplinary Sciences: Computational Life Sciences, 5(4), 274-279.
66. Patidar, K., Panwar, U., Vuree, S., Sweta, J., Sandhu, M. K., Nayarisseri, A., & Singh, S. K. (2019). An in silico approach to identify high affinity small molecule targeting m-TOR inhibitors for the clinical treatment of breast cancer. Asian Pacific journal of cancer prevention: APJCP, 20(4), 1229.
67. Prajapati, L., Khandelwal, R., Yogalakshmi, K. N., Munshi, A., & Nayarisseri, A. (2020). Computer-aided Structure prediction of Bluetongue Virus coat protein VP2 assisted by Optimized Potential for Liquid Simulations (OPLS). Current topics in medicinal chemistry, 20(19), 1720-1732.
68. Udhwani, T., Mukherjee, S., Sharma, K., Sweta, J., Khandekar, N., Nayarisseri, A., & Singh, S. K. (2019). Design of PD-L1 inhibitors for lung cancer. Bioinformation, 15(2), 139.]
69. Vuree, S., Dunna, N.R., Khan, I.A., Alharbi, K.K., Vishnupriya, S., Soni, D., Shah, P., Chandok, H., Yadav, M. and Nayarisseri, A. (2013). Pharmacogenomics of drug resistance in Breast Cancer Resistance Protein (BCRP) and its mutated variants. journal of pharmacy research, 6(7), 791-798
70. Nayarisseri, A., & Singh, S. K. (2019). Functional inhibition of VEGF and EGFR suppressors in cancer treatment. Current topics in medicinal chemistry, (3), 178-179.
71. Nayarisseri, A., & Yadav, M. (2015). Editorial (Thematic Issue: Mechanistics in drug design-experimental molecular biology vs. molecular modeling). Current topics in medicinal chemistry,

15(1), 3-4.

72. Nayarisseri, A., Khandelwal, R., Madhavi, M., Selvaraj, C., Panwar, U., Sharma, K., Hussain, T. and Singh, S.K. (2020). Shape-based machine learning models for the potential novel COVID-19 protease inhibitors assisted by molecular dynamics simulation. Current topics in medicinal chemistry, 20(24), 2146-2167.
73. Nayarisseri, A., Khandelwal, R., Tanwar, P., Madhavi, M., Sharma, D., Thakur, G., Speck-Planche, A. and Singh, S.K. (2021). Artificial intelligence, big data and machine learning approaches in precision medicine & drug discovery. Current drug targets, 22(6), 631-655.
74. Nayarisseri, A. (2020). Most promising compounds for treating covid-19 and recent trends in antimicrobial & antifungal agents. Current topics in medicinal chemistry, 20(24), 2119-2125.
75. Suryanarayanan, V., Panwar, U., Chandra, I., & Singh, S. K. (2018). De novo design of ligands using computational methods. In Computational Drug Discovery and Design (pp. 71-86). Humana Press, New York, NY.
76. Aarthy, M., Panwar, U., & Singh, S. K. (2020). Structural dynamic studies on identification of EGCG analogues for the inhibition of Human Papillomavirus E7. Scientific reports, 10(1), 1-24.
77. Panwar, U., & Singh, S. K. (2018). An overview on Zika Virus and the importance of computational drug discovery. Journal of Exploratory Research in Pharmacology, 3(2), 43-51.
78. Aarthy, M., & Singh, S.K., 2021. Interpretations on the Interaction between Protein Tyrosine Phosphatase and E7 Oncoproteins of High and Low-Risk HPV: A Computational Perception. ACS Omega, 6(25), pp.16472–16487.
79. Selvaraj, C., Panwar, U., Dinesh, DC., Bouřa, E., Sing, P., Dubey, V.K., Singh, S.K., 2021. Microsecond MD Simulation and Multiple-Confirmation Virtual Screening to Identify Potential Anti-COVID-19 Inhibitors Against SARS-CoV-2 Main Protease. Frontiers in Chemistry , 8, 595273.
80. Selvaraj, C., Dinesh, DC., Panwar, U., Bouřa, E., Singh, S.K., 2021. High-Throughput Screening and Quantum Mechanics for Identifying Potent Inhibitors against Mac1 Domain of SARS-CoV-2 Nsp3. IEEE/ACM Transactions on Computational Biology and Bioinformatics , 18(4), pp.1262-1270.
81. Selvaraj C., Selvaraj G., Ismail RM.,Baazeem A., Wei DQ., Singh, S.K., 2021. Interrogation of Bacillus anthracis SrtA active site loop forming open/close lid conformations through extensive MD simulations for understanding binding selectivity of SrtA inhibitors. Saudi Journal of Biological Sciences, 28(7), pp.3650-3659.
82. Basak, S. C., Nayarisseri, A., González-Díaz, H., &Bonchev, D. (2016). Editorial (Thematic Issue: chemoinformatics models for pharmaceutical design, part 1). 22(33):5041-5042.
83. Basak, S. C., Nayarisseri, A., González-Díaz, H., &Bonchev, D. (2016). Editorial (Thematic Issue: Chemoinformatics models for pharmaceutical design, part 2). 22(34):5177-5178.
84. Chandrakar, B., Jain, A., Roy, S., Gutlapalli, V.R., Saraf, S., Suppahia, A., Verma, A., Tiwari, A., Yadav, M. and Nayarisseri, A. (2013). Molecular modeling of Acetyl-CoA carboxylase (ACC) from Jatropha curcas and virtual screening for identification of inhibitors. journal of pharmacy research, 6(9), 913-918.

85. Gokhale, P., Chauhan, A. P. S., Arora, A., Khandekar, N., Nayarisseri, A., & Singh, S. K. (2019). FLT3 inhibitor design using molecular docking based virtual screening for acute myeloid leukemia. Bioinformation, 15(2), 104.
86. Kleandrova, V. V., Scotti, M. T., Scotti, L., Nayarisseri, A., & Speck-Planche, A. (2020). Cell-based multi-target QSAR model for design of virtual versatile inhibitors of liver cancer cell lines. SAR and QSAR in Environmental Research, 31(11), 815-836.
87. Marunnan, S. M., Pulikkal, B. P., Jabamalairaj, A., Bandaru, S., Yadav, M., Nayarisseri, A., & Doss, V. A. (2017). Development of MLR and SVM aided QSAR models to identify common SAR of GABA uptake herbal inhibitors used in the treatment of Schizophrenia. Current neuropharmacology, 15(8), 1085-1092.
88. Mendonça-Junior, F. J., Scotti, M. T., Nayarisseri, A., Zondegoumba, E. N., & Scotti, L. (2019). Natural bioactive products with antioxidant properties useful in neurodegenerative diseases. Oxidative medicine and cellular longevity, 2019.
89. Mukherjee, S., Abdalla, M., Yadav, M., Madhavi, M., Bhrdwaj, A., Khandelwal, R., Prajapati, L., Panicker, A., Chaudhary, A., Albrakati, A. and Hussain, T. (2022). Structure-Based Virtual Screening, Molecular Docking, and Molecular Dynamics Simulation of VEGF inhibitors for the clinical treatment of Ovarian Cancer. Journal of Molecular Modeling, 28(4), 1-21.
90. Natchimuthu, V., Bandaru, S., Nayarisseri, A., & Ravi, S. (2016). Design, synthesis and computational evaluation of a novel intermediate salt of N-cyclohexyl-N-(cyclohexylcarbamoyl)-4-(trifluoromethyl) benzamide as potential potassium channel blocker in epileptic paroxysmal seizures. Computational biology and chemistry, 64, 64-73.
91. Nayarisseri A, Khandelwal R, Tanwar P, Madhavi M, Sharma D, Thakur G, Speck-Planche A, Singh SK. Artificial Intelligence, Big data and Machine Learning approaches in Precision Medicine & Drug Discovery. Curr Drug Targets. 22(6):631-655.
92. Nayarisseri, A. (2019). Prospects of utilizing computational techniques for the treatment of human diseases. Current topics in medicinal chemistry, 19(13), 1071-1074.
93. Nayarisseri, A. (2020). Experimental and computational approaches to improve binding affinity in chemical biology and drug discovery. Current Topics in Medicinal Chemistry, 20(19), 1651-1660.
94. Panwar, U., Singh, S.K., 2021. In silico virtual screening of potent inhibitor to hamper the interaction between HIV-1 integrase and LEDGF/p75 interaction using E-pharmacophore modeling, molecular docking, and dynamics simulations. Computational Biology and Chemistry, 93, 107509.
95. Panwar, U., Singh, S.K., 2021. Atom-based 3D-QSAR, molecular docking, DFT, and simulation studies of acylhydrazone, hydrazine, and diazene derivatives as IN-LEDGF/p75 inhibitors. Structural Chemistry , 32, pp.337–352
96. Kundu, D., Selvaraj, C., Singh, S.K., Dubey, V.K. Singh, S.K., 2020. Identification ofnew anti-CoV drug chemical compounds from Indian spices exploiting SARS-CoV-2 main protease as target. Journal of Biomolecular Structure and Dynamics. 39(9), 3428-3434.

97. Pradiba, D., Aarthy, M., Shunmugapriya, V., Singh, S. K., & Vasanthi, M. (2018). Structural insights into the binding mode of flavonols with the active site of matrix metalloproteinase-9 through molecular docking and molecular dynamic simulations studies. Journal of Biomolecular Structure and Dynamics, 36(14), 3718-3739.
98. Sharda, S., Sarmandal, P., Cherukommu, S., Dindhoria, K., Yadav, M., Bandaru, S., Sharma, A., Sakhi, A., Vyas, T., Hussain, T. and Nayarisseri, A. (2017). A virtual screening approach for the identification of high affinity small molecules targeting BCR-ABL1 inhibitors for the treatment of chronic myeloid leukemia. *Current topics in medicinal chemistry*, *17*(26), 2989-2996.
99. Tripathi, S. K., Selvaraj, C., Singh, S. K., & Reddy, K. K. (2012). Molecular docking, QPLD, and ADME prediction studies on HIV-1 integrase leads. *Medicinal Chemistry Research*, *21*(12), 4239-4251.
100. Vijayalakshmi, P., Selvaraj, C., Singh, S. K., Nisha, J., Saipriya, K., & Daisy, P. (2013). Exploration of the binding of DNA binding ligands to Staphylococcal DNA through QM/MM docking and molecular dynamics simulation. Journal of Biomolecular Structure and Dynamics, 31(6), 561-571.
101. Panwar, U., & Singh, S. K. (2018). Structure-based virtual screening toward the discovery of novel inhibitors for impeding the protein-protein interaction between HIV-1 integrase and human lens epithelium-derived growth factor (LEDGF/p75). Journal of Biomolecular Structure and Dynamics, 36(12), 3199-3217.
102. Selvaraj, C., Krishnasamy, G., Jagtap, S. S., Patel, S. K., Dhiman, S. S., Kim, T. S., ... & Lee, J. K. (2016). Structural insights into the binding mode of d-sorbitol with sorbitol dehydrogenase using QM-polarized ligand docking and molecular dynamics simulations. Biochemical Engineering Journal, 114, 244-256.
103. Singh, S., Vijaya Prabhu, S., Suryanarayanan, V., Bhardwaj, R., Singh, S. K., & Dubey, V. K. (2016). Molecular docking and structure-based virtual screening studies of potential drug target, CAAX prenyl proteases, of Leishmania donovani. Journal of Biomolecular Structure and Dynamics, 34(11), 2367-2386.
104. Selvaraj, C., Sivakamavalli, J., Vaseeharan, B., Singh, P., & Singh, S. K. (2014). Structural elucidation of SrtA enzyme in Enterococcus faecalis: an emphasis on screening of potential inhibitors against the biofilm formation. Molecular BioSystems, 10(7), 1775-1789.
105. Shafreen, R. M. B., Selvaraj, C., Singh, S. K., & Pandian, S. K. (2013). Exploration of fluoroquinolone resistance in Streptococcus pyogenes: comparative structure analysis of wild-type and mutant DNA gyrase. Journal of Molecular Recognition, 26(6), 276-285.
106. Bandaru, S., Marri, V.K., Kasera, P., Kovuri, P., Girdhar, A., Mittal, D.R., Ikram, S., Gv, R. and Nayarisseri, A. (2014). Structure based virtual screening of ligands to identify cysteinyl leukotriene receptor 1 antagonist. Bioinformation, 10(10), 652.
107. Yang, H., Lou, C., Sun, L., Li, J., Cai, Y., Wang, Z., Li, W., Liu, G. and Tang, Y. (2019). admetSAR 2.0: web-service for prediction and optimization of chemical ADMET properties. Bioinformatics, 35(6), 1067-1069.

Figures

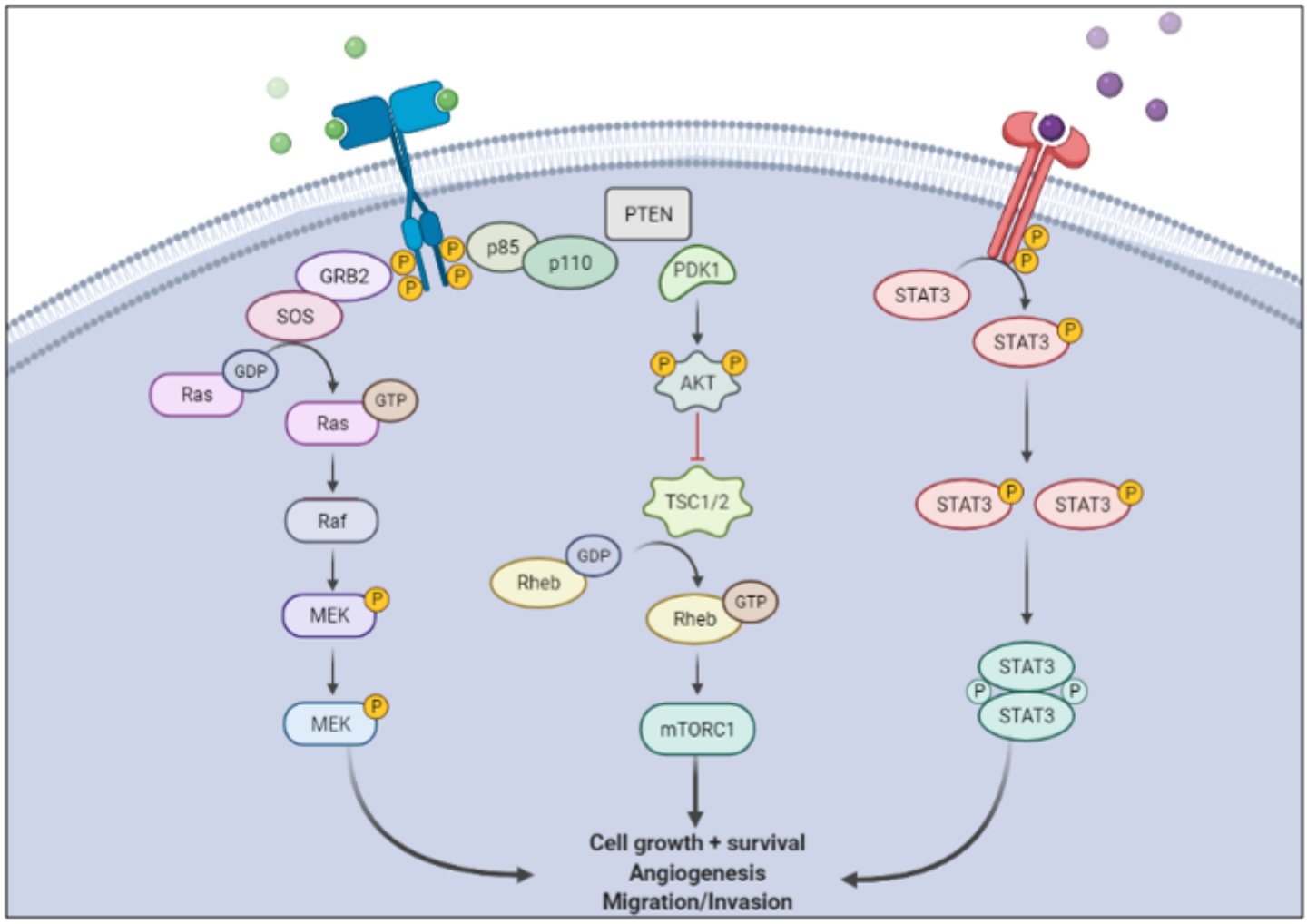

Figure 1

EGFRvIII and STAT signaling in glioblastoma cell.

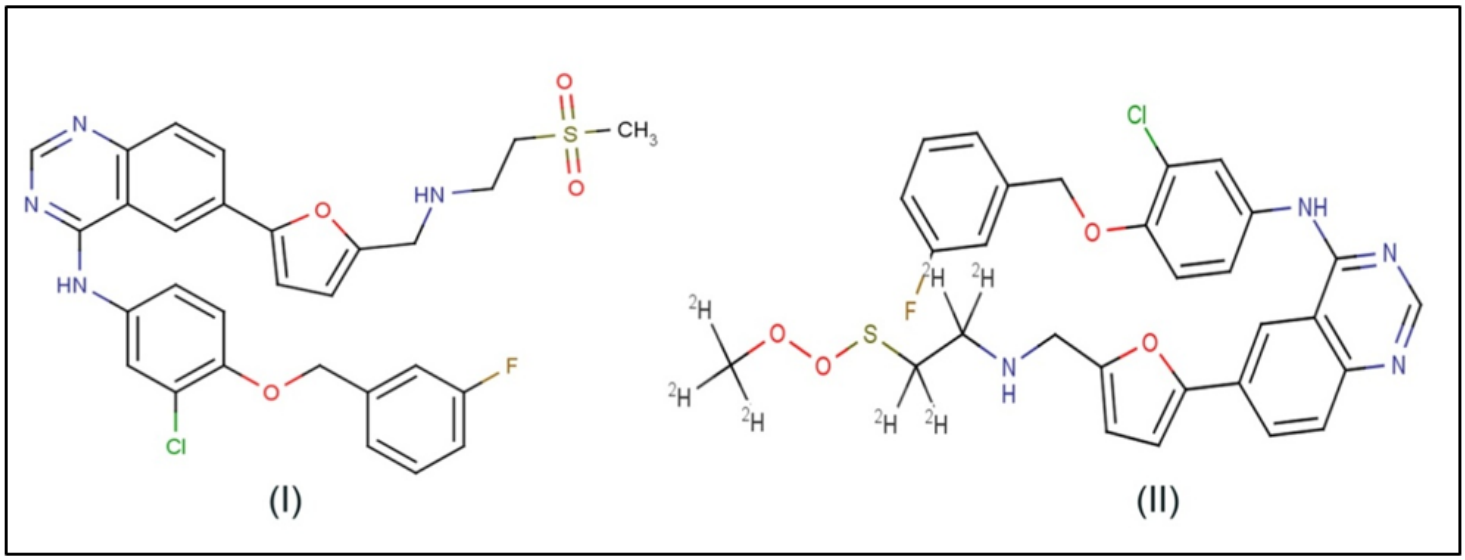

Figure 2

(I) PubChem ID: 208908, the most effective established compound obtained from Molecular docking. (II) PubChem ID: 59671768, the most effective virtual screened compound obtained from Virtual screening from PubChem database

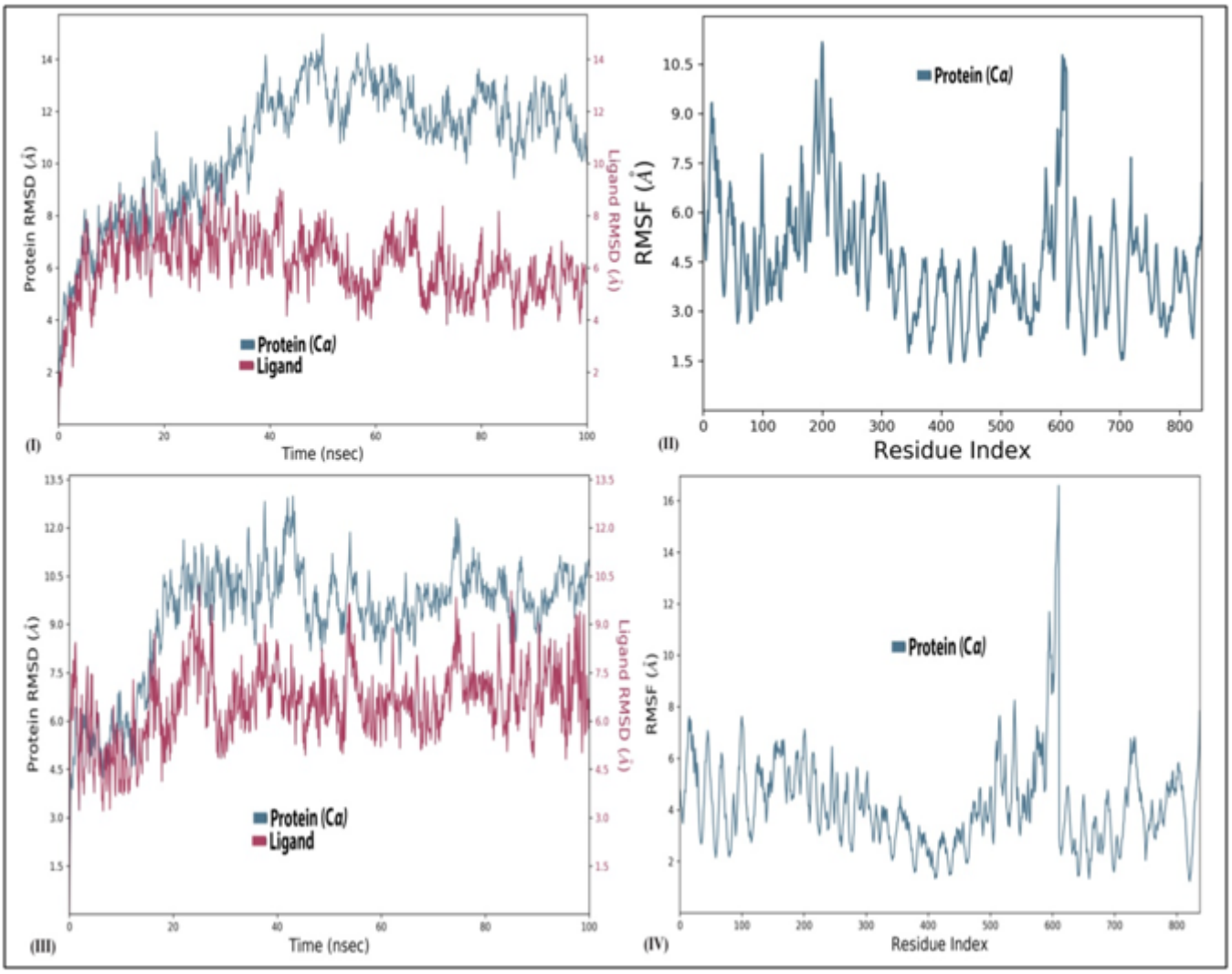

Figure 3

Molecular dynamics RMSD and RMSF of free EGFR: (I,II) - EGFR complex with best established compound PubChem ID: 208908, (III,IV) - EGFR complex with the best virtual screened compound PubChem ID: 59671768.

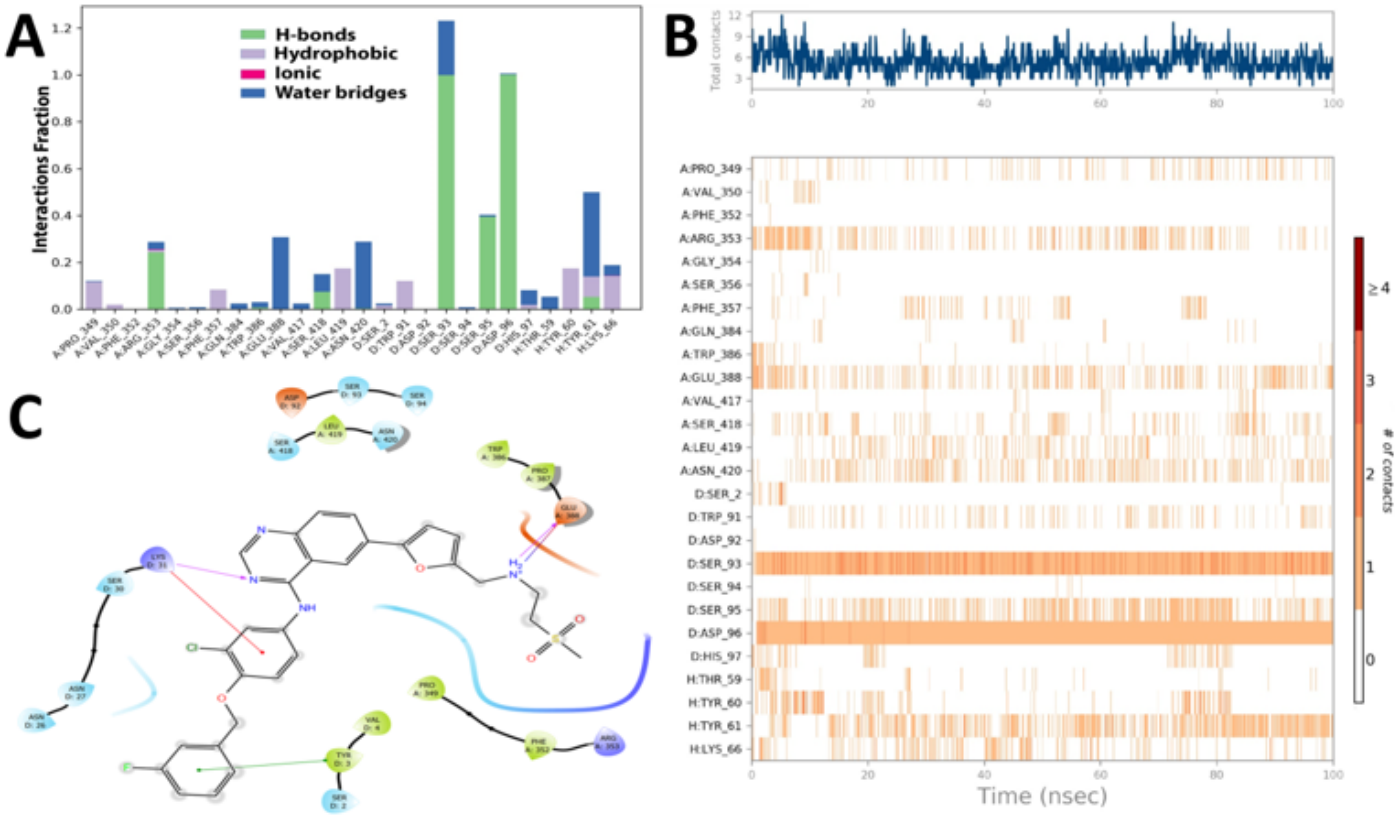

Figure 4

Interaction diagram of EGFR complex with best-established compound PubChem ID: 59671768 observed during the molecular dynamic's simulation. (A) The protein-ligand interaction profile. (B) Residues interact with the ligand in each trajectory frame. (C) Representation of 2D diagram of a protein-ligand complex, [2D interaction graph color notification for bonding: Pink Color – hydrogen bonding, Red & Green– Pi-Pi interaction, Reddish Blue - Salt & Water Bridge]

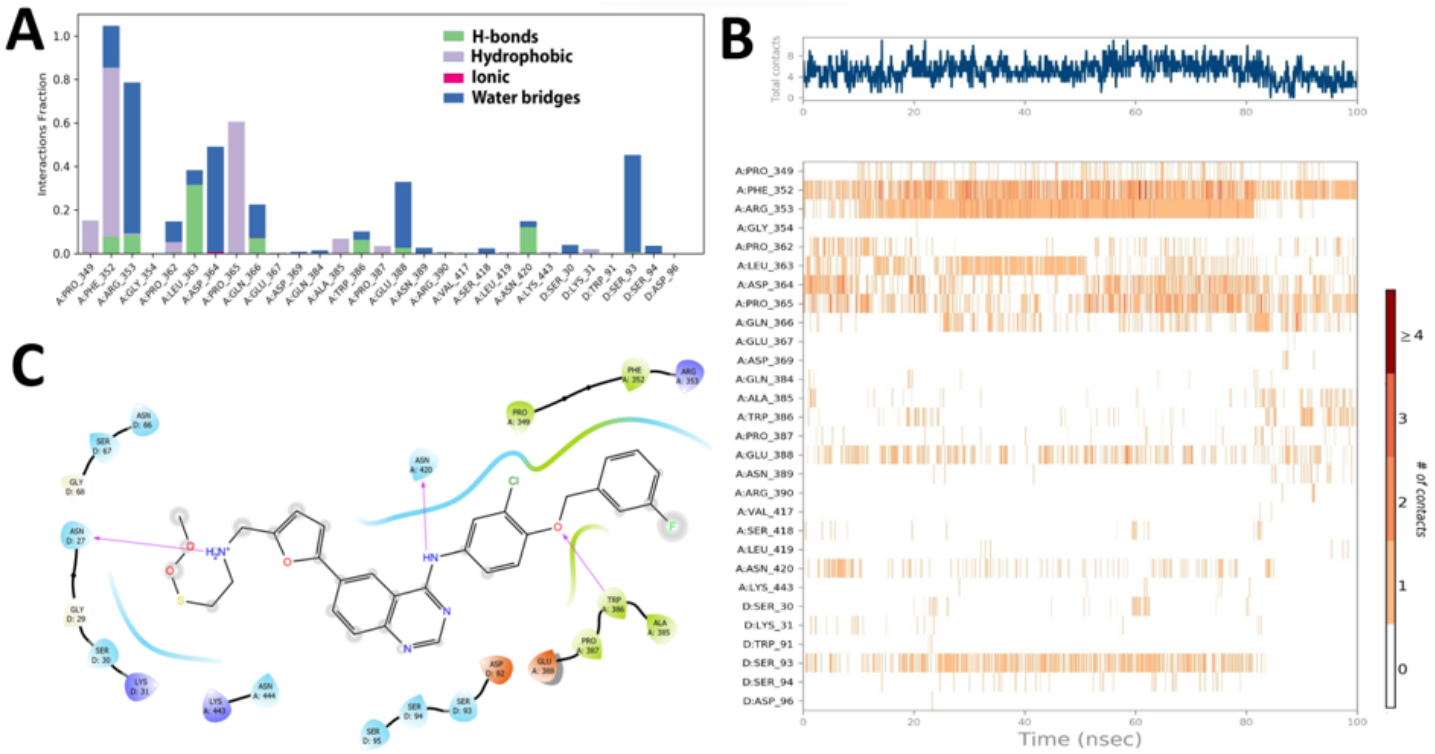

Figure 5

The ligand property trajectory of the EGFR complex with best established compound Lapatinib (PubChem ID: 208908) during the 100 ns simulation.

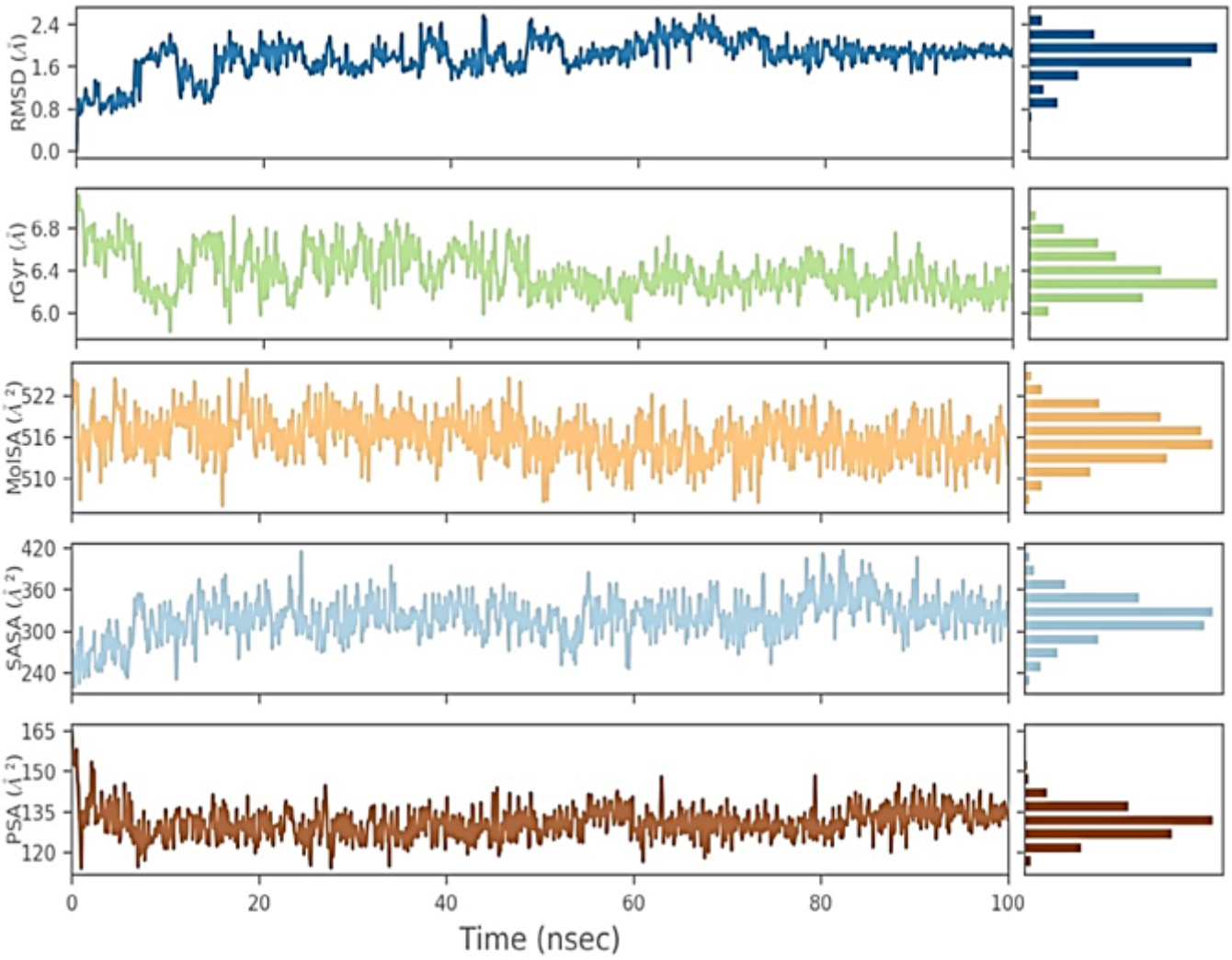

Figure 6

The ligand property trajectory of the EGFR complex with the best virtual screened compound (PubChem ID: 59671768) during the 100 ns simulation.

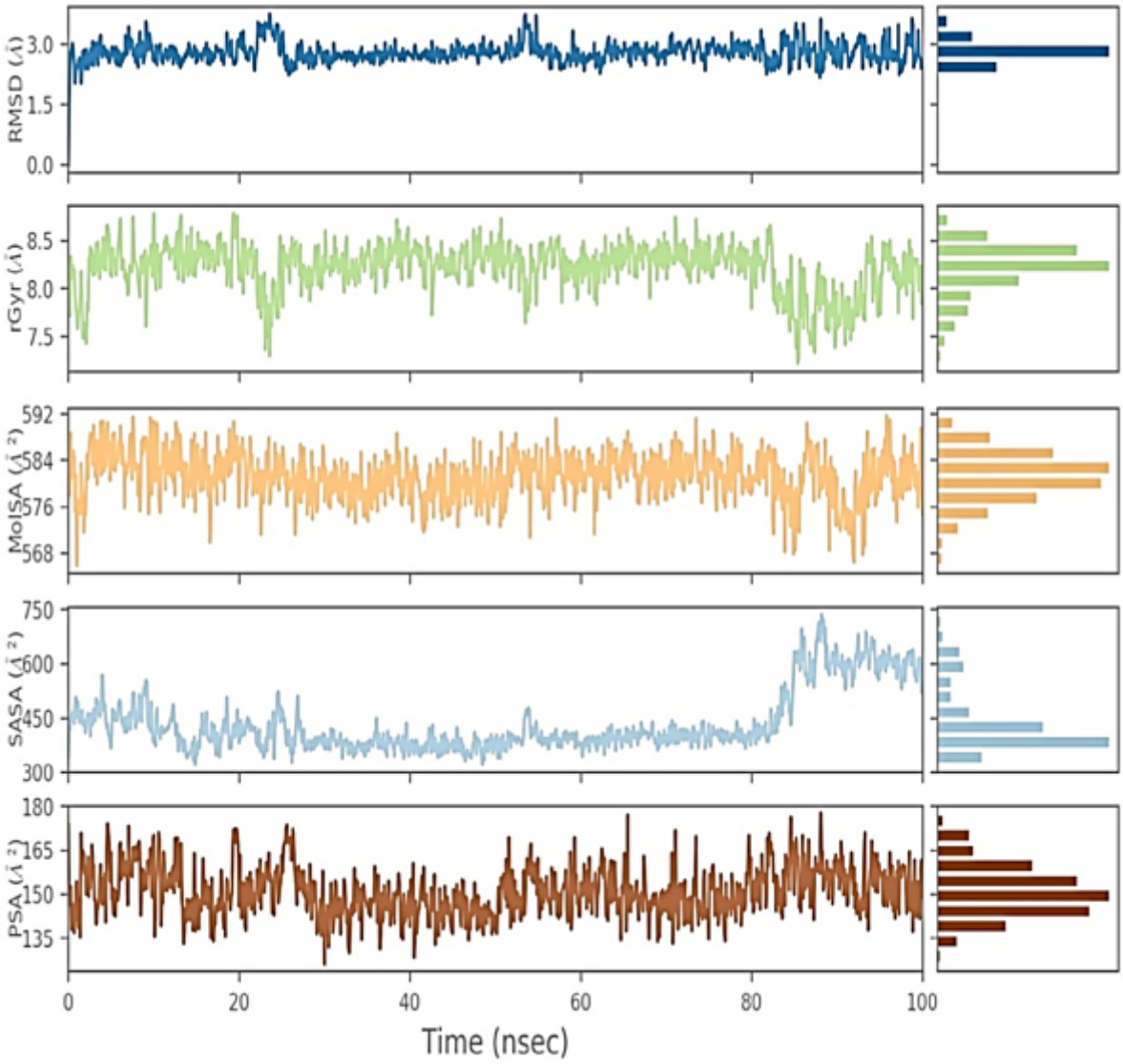

Figure 7

3D visualization H-bond interaction of established compound (PubChem ID: 208908) and virtually screened compound (PubChem ID: 59671768) with EGFR.

[Cyan Color – Residues, Purple Color – Ligand, Green Dotted Lines – Hydrogen bonding, Black Dotted Lines – Pi-Pi interaction, Pink Dotted Lines – Salt Bridge, Chain Differentiation – Orange & red]

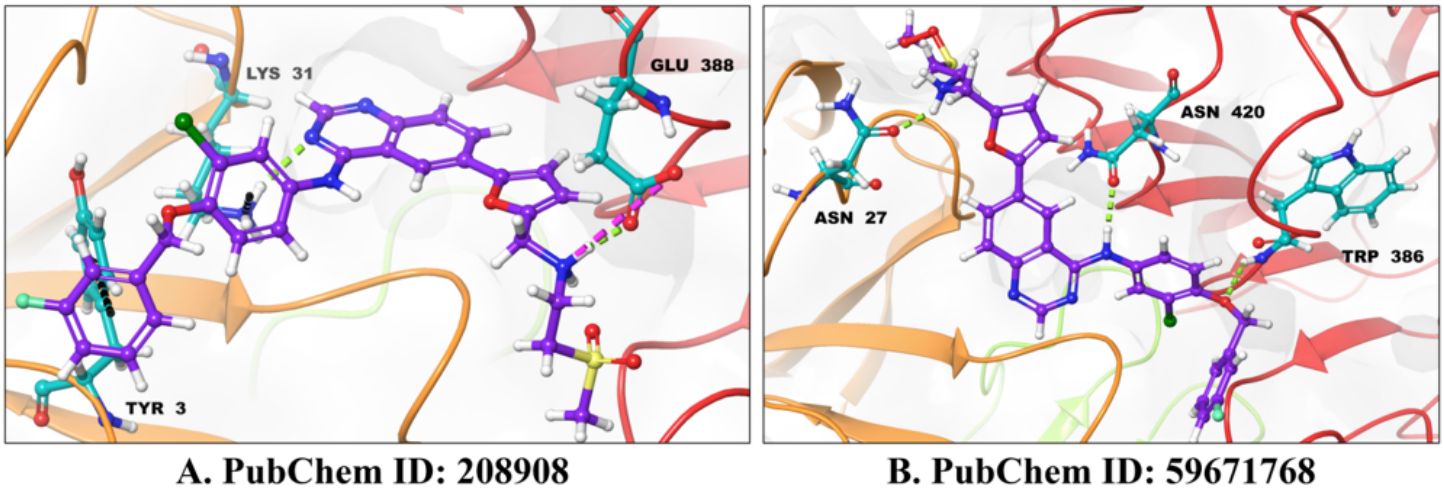

Figure 8

Graphical representation of comparative study among two best virtual screened compounds and two best-established compounds.

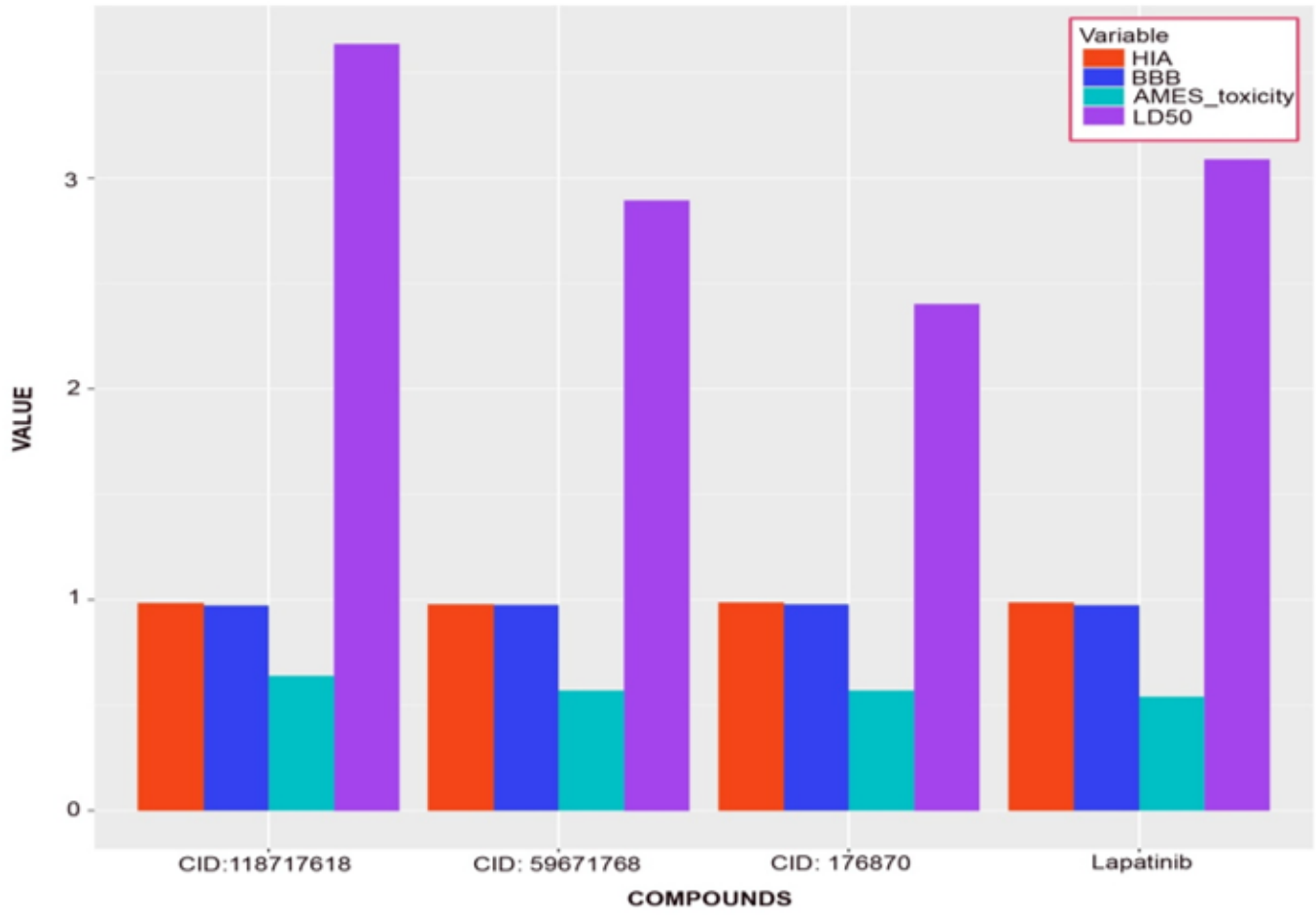

Figure 9

Boiled egg plot of the best established (PubChem ID: 208908) and the best virtually screened compound (Pub CID: 59671768).

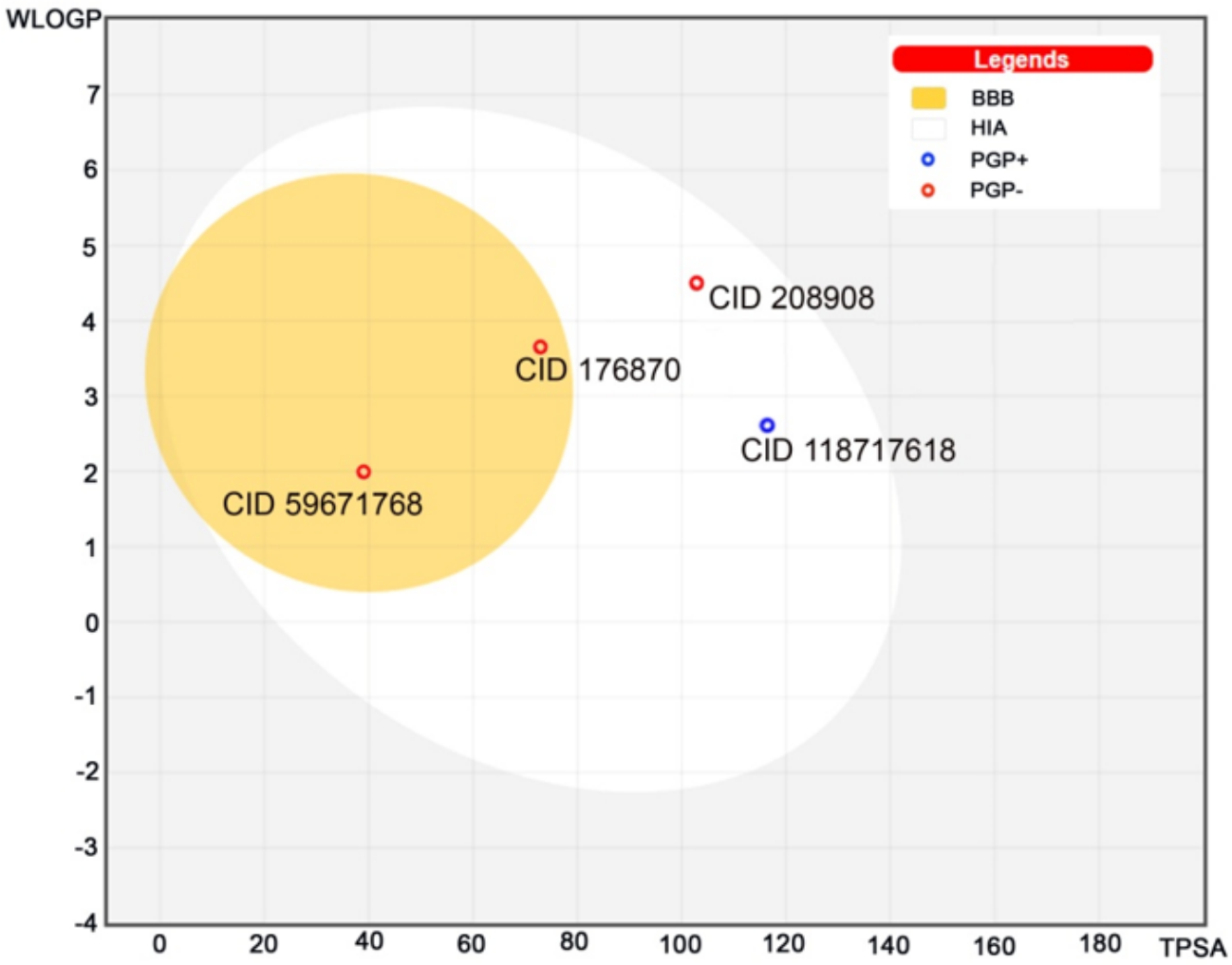

Figure 10

Adsorption analysis of the four compounds.

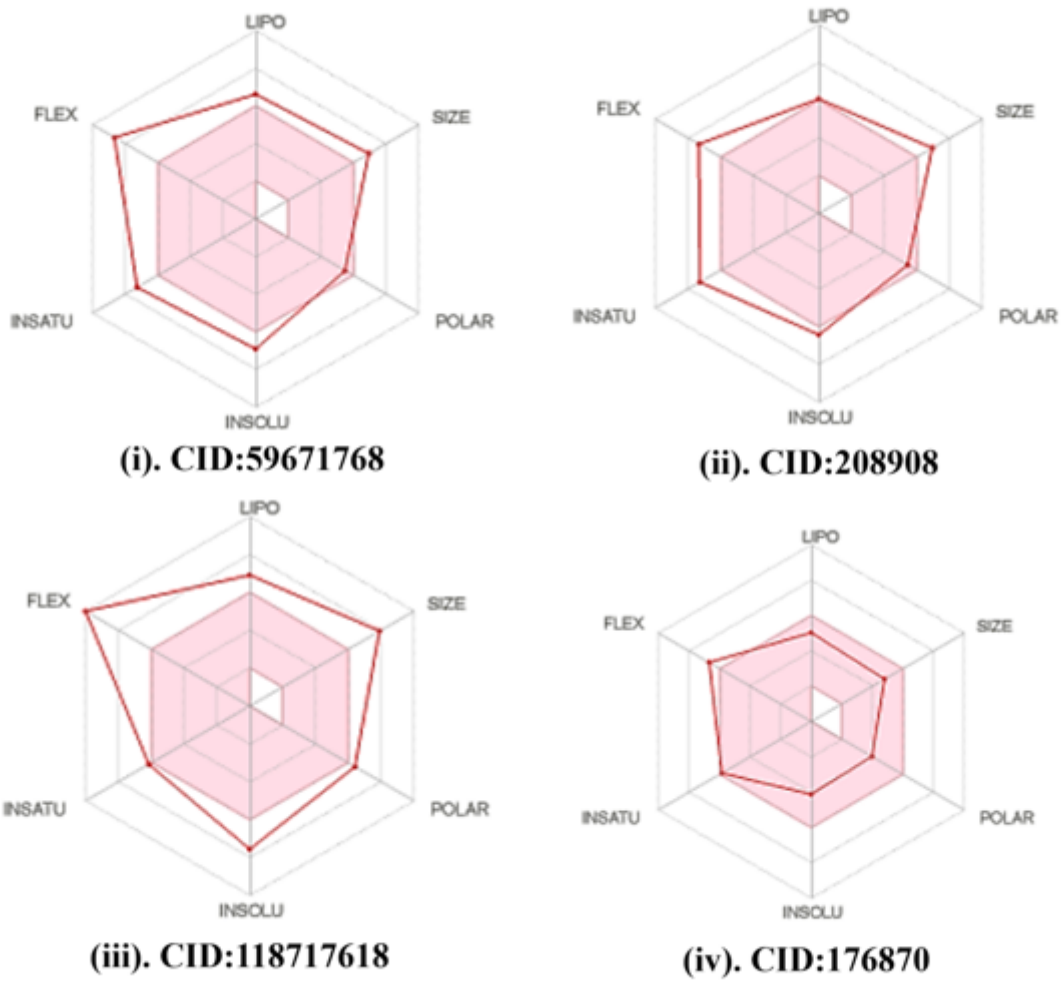

Figure 11

Adsorption analysis of the four compounds.